Carlsberg Res. Commun. Vol. 50, p. 43–72, 1985

HUMAN MEIOSIS IX. CROSSING OVER AND CHIASMA FORMATION IN OOCYTES

by

MAJA BOJKO

Department of Physiology, Carlsberg Laboratory, Gamle Carlsberg Vej 10, DK-2500 Copenhagen Valby

Keywords: Human female meiosis, synaptonemal complex, recombination nodule, bar

Human oocytes from foetal ovaries have been analyzed by serial sectioning and three dimensional reconstruction from electron micrographs. Analysis of five late zygotene, twenty pachytene, four early and three mid diplotene nuclei allowed the following observations and conclusions: 1) Nuclei at pachytene can by morphological criteria be allocated into three substages. 2) The synaptonemal complex complement is twice as long in the oocytes as in the spermatocytes. 3) The total number of nodules decreases from a mean of 68 at late zygotene to a mean of 30 at early diplotene. During pachytene, an increasing number of nodules transforms into bars. A mean of 6 bars was observed in late zygotene nuclei compared to a mean of 17 at late pachytene. 4) Nodules and bars are distributed nonrandomly among the bivalents and bivalent arms. The observed frequency of bivalents devoid of recombination structures is only between one- and two-thirds of the frequency expected if nodules were distributed at random. 5) The distribution of recombination structures along the bivalent arms is not uniform. More nodules and bars than expected from a random distribution are located in the vicinity of telomeres. Comparison of neighbour nodule/bars distances at different substages of pachytene indicated that the elimination of recombination structures primarily affects nodules and bars close to each other. 6) The distribution of recombination structures along the individual bivalents was uneven, regions with high frequency of recombination nodules and bars alternating with regions of low frequency. This pattern is very similar to that reported for human spermatocytes, which indicates the same distribution of crossovers in the two sexes. 7) Elimination of the synaptonemal complex starts at early diplotene at a limited number of sites until about 68 intact segments are created. 8) Chiasmata are not morphologically recognizable after the elimination of the synaptonemal complex is completed at mid diplotene.

1. INTRODUCTION

Sex differences in the frequency of meiotic crossing over have been reported from a few animal species (2, 6, 12). In man, the frequency of recombination has been reported to be 1.5 times higher in the female than in the male between the LA and FOUR loci in the HL-A histocompatibility system (29) and from 1.5 to 2 times higher between the Secretor and Lutheran loci (11). Analysis of chiasmata in diakinesis nuclei of oocytes and spermatocytes has, however, not confirmed such a difference. In a culture of human oocytes, a mean of 43.5 chiasmata per nucleus was reported by JAGIELLO et al. (24) from an analysis of 621 diakinesis/metaphase I bivalents, and between 37 and 48 chiasmata per nucleus were observed in 15 oocytes matured in vitro (13). Corresponding chiasma counts in the human male are decidedly higher: HULTÉN (23) found a mean of 50.6 (range 43-60) chiasmata in 41 nuclei, and 51.9 chiasmata per cell were inferred by analyzing bivalents from 297 spermatocytes (14).

Observations in a variety of organisms have suggested that the number and distribution of crossovers can be assessed through an analysis of the recombination nodules (7), small, dense bodies associated with the central region of the

Springer-Verlag 0105-1938/85/0050/0043/$06.00

synaptonemal complex during zygotene and pachytene (31). The evidence in support of this proposal can be summarized as follows: 1) The number and distribution of recombination nodules among bivalents correspond fairly well with that of meiotic exchanges and/or chiasmata in a number of different species (see 8, 28, 31 for reviews). 2) In Bombyx, where crossing over is limited to the male, these structures are only present in the male, although both sexes have normal chromosome pairing with regular synaptonemal complex formation (18, 26). 3) The meiotic mutants mei-41 and mei-218 of Drosophila show a parallel decrease in recombination frequency and the number of recombination nodules (8). 4) Autoradiographic analysis in Drosophila females have demonstrated DNA synthesis in the vicinity of the recombination nodules (10). 5) Reconstructed nuclei from the male Bombyx and the basidiomycete Coprinus cinereus, covering the period from zygotene to metaphase I, have shown the morphological continuity between recombination nodules and chiasmata (18, 22).

The number and distribution of crossovers in human spermatocytes was assessed in a recent analysis on recombination nodules and bars (19, 20, 21, 27). These studies suggest that crossing over occurred perferentially at mid pachytene and was characterized by a morphological transition of spherical recombination nodules into bars. However, additional crossing over seems to take place during early and late pachytene, since the number of bars at mid pachytene was considerably below the number of chiasmata at diakinesis. The distribution of crossovers was estimated by cumulating the distribution of bars at early pachytene and distribution of nodules and bars at mid and late pachytene. The cumulated distribution showed that the frequency of crossovers displayed a characteristic pattern of peaks and troughs along the bivalent arms.

In this paper the number and distribution of recombination nodules and bars have been determined in oocytes and compared with that reported in spermatocytes (20) in order to investigate whether sex specific differences in crossing over can account for the reported differences in chiasma counts. Since the synaptonemal complexes in the female are twofold longer than in the male (5) one can assess a possible effect of the synaptonemal complex length on the number and distribution of crossover events.

2. MATERIALS AND METHODS

2.1. Materials

The material consists of 32 nuclei from the same foetal ovaries as those used previously (5). One late zygotene nucleus (no. 2) was from a 24-26 week old foetus, four pachytene nuclei (nos. 12 and 14-16) were from a 16-17 week old foetus and the rest from a 22-24 week old foetus.

In this study, the synaptonemal complex com-

Table I.
Percent of nuclei displaying different morphological features at late zygotene and early, mid and late pachytene. n, number of nuclei.

Stage	Spherical shape	Nucleolus type A	B	C	Distinct secondary constriction	Electron dense region in centromere
Late zygotene n = 5	20	40	20	40	80	20
Early pachytene n = 8	13	13	75	13	38	38
Mid pachytene n = 6	0	33	33	33	50	66
Late pachytene n = 7*	86	14	29	57	0	86

*Data for one of the early diplotene nuclei (no. 26) with nearly intact synaptonemal complexes is included.

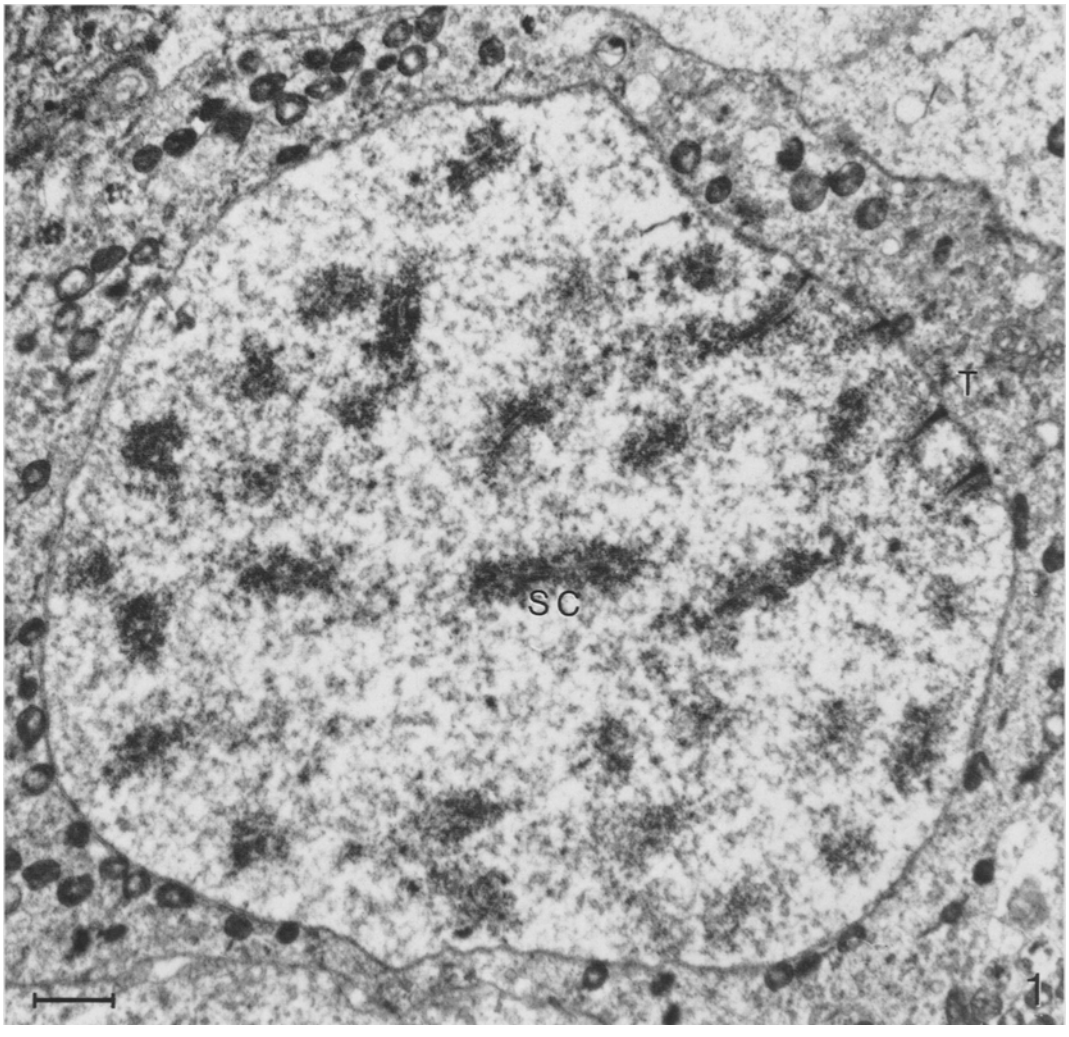

Figure 1. Survey micrograph of an early pachytene nucleus. The telomeres (T) are aggregated into one area on the nuclear envelope. Note the irregular shape of the nucleus. SC, synaptonemal complex. (Bar = 1 μm).

plements of five late zygotene nuclei (nos. 1-5), twenty pachytene (nos. 6-25) and two early diplotene nuclei (nos. 26 and 27) were completely reconstructed. In addition, two early diplotene nuclei (nos. 28 and 29) and three mid diplotene nuclei (nos. 30-32) were serially sectioned and partially reconstructed.

2.2. Methods

The procedures used for fixation, serial sectioning, staining, electron microscopy and the subsequent reconstruction of the chromosome complement, as well as the computerized methods for measuring the length of the synaptonemal complexes have been described previously (5, 27).

3. RESULTS

3.1. Substages of pachytene

Five of the investigated nuclei (nos. 1-5) were at the late zygotene stage as evidenced by the presence of short stretches (less than 3% of the

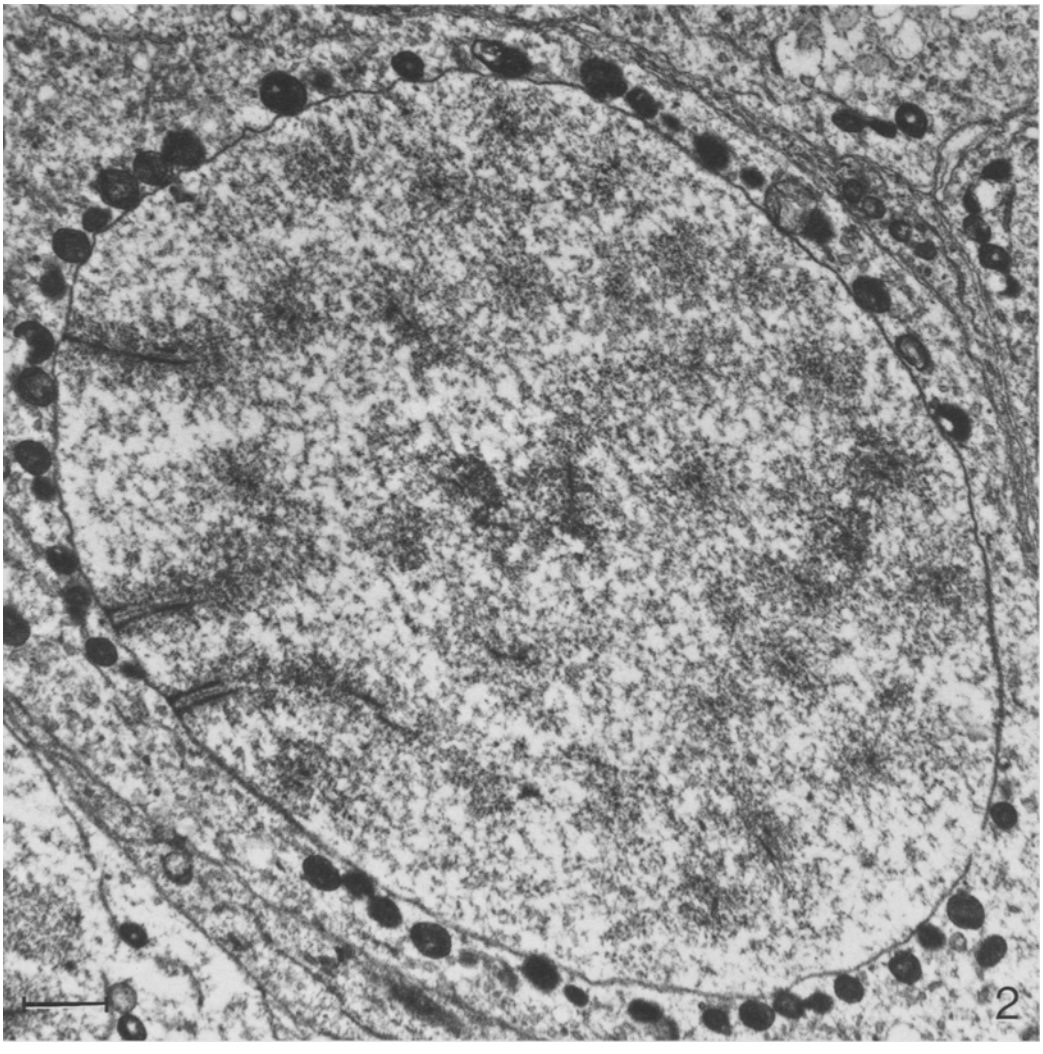

Figure 2. Survey micrograph of a mid pachytene nucleus. Note that the chromatin along the synaptonemal complex is dispersed and evenly distributed in the nucleus. Note the mitochondia closely surrounding the nuclear envelope. (Bar = 1 μm).

complement) of unpaired lateral components and the aggregation of the telomere attachment sites within a limited area on the nuclear envelope giving rise to a chromosome bouquet.

The 20 pachytene nuclei were allocated to an early, a mid and a late pachytene stage using the distribution of the telomeres on the nuclear envelope as the criterium. Eight nuclei (nos. 6-11 and 13-14) displaying a prominent bouquet were classified as early pachytene, six nuclei (nos. 12 and 15-19) with a dissolving bouquet as mid pachytene, and six nuclei (nos. 20-25), with telomeres distributed evenly on the nuclear envelope were assigned to late pachytene. The morphological development of nuclear structures during pachytene was not sufficiently synchronous to warrant a further temporal subdivision, as has been described for spermatocytes (19).

As can be seen in Table I the morphology of

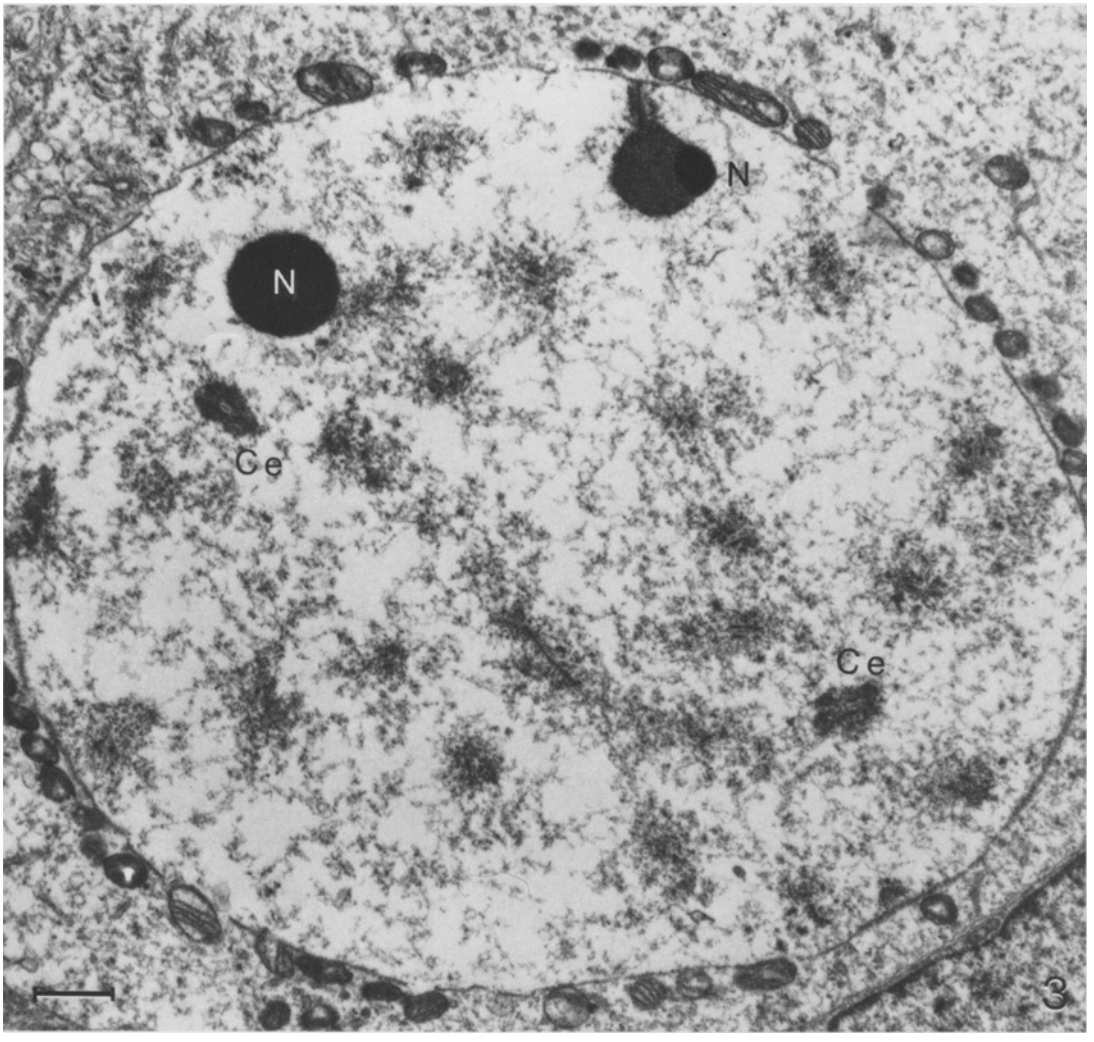

Figure 3. Survey micrograph of a late pachytene nucleus. Ce, centromere chromatin. N, nucleolus. (Bar = 1 µm).

four nuclear structures changed in relation to the three pachytene substages.

1) From zygotene to mid pachytene the nuclei are irregular - kidney, heart or egg shaped (Figures 1 and 2), whereas spherical nuclei predominate at late pachytene (Figure 3).

2) Three types of nucleoli are observed at pachytene: Type A are irregularly shaped, of high electron density and contain branched electron transparent cavities (Figure 4a). Type B are spherical nucleoli with electron transparent cavities (Figure 4b). Type C are compact, spherical, electron dense nucleoli (Figure 4c). In all types of nucleoli the association with acrocentric bivalents is mediated by the fibrillar body of medium electron density. At zygotene, nucleoli of the three types were observed with equal frequency (5). During pachytene, however, a successive transition from type B to type C is evident from the frequencies given in Table I.

3) The centromeric chromatin at late zygotene is only slightly more condensed than the flanking chromatin and its outline is irregular (5). During early pachytene, the chromatin of

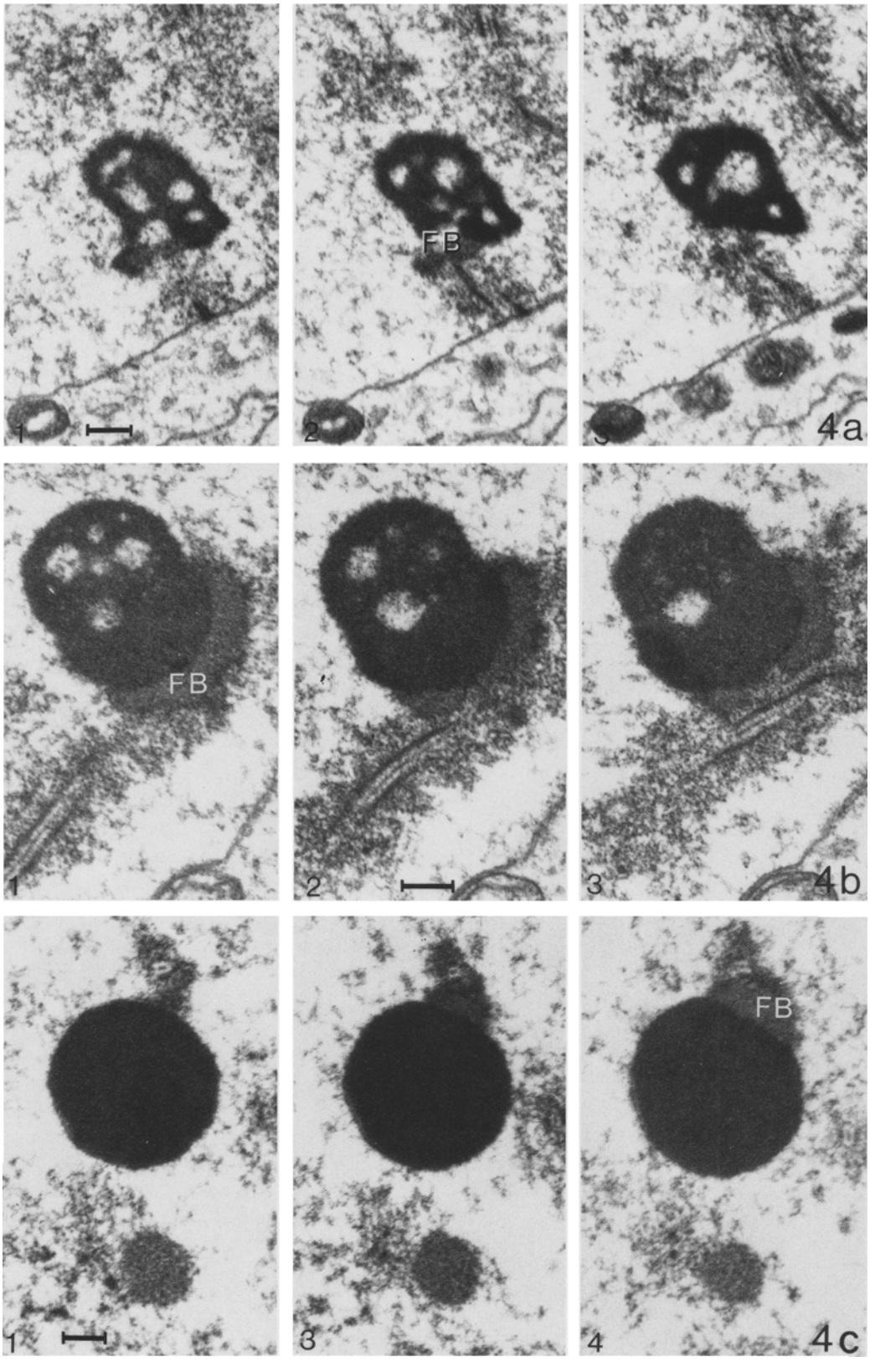
FB
1
2
4a
FB
1
2
3
4b
FB
1
3
4
4c

Figure 4. Nucleoli of different morphology from early pachytene (Figures 4a and b) and late pachytene (Figure 4c) oocytes. FB, fibrillar body. The numbers are the relative section numbers for the short series of consecutive sections. (Bars = 0.5 μm).

the centromere region becomes more distinct and forms in the majority of the nuclei a homogeneous, condensed spherical body around the synaptonemal complex. During mid and late pachytene domains of high electron density develop in the centromeric chromatin (Figure 5).

4) The secondary constrictions on chromosomes 1, 9 and 16 in most late zygotene and early pachytene nuclei form a distinct, dimorphic body, which consists of a well-defined matrix containing a number of compact knobs (Figure 6a). During pachytene, the matrix and the knobs become less distinct (Figure 6b), and eventually the constriction is recognizable only by the presence of a few small knobs (Figure 6c).

Table II presents the total complement lengths in the 20 nuclei at the three pachytene substages. Data for one of the early diplotene nuclei (no. 26) with nearly intact synaptonemal complexes is pooled with the late pachytene data. The lengths appear to be roughly constant throughout pachytene and similar to those reported previously (5) for mid and late zygotene oocyte nuclei (465 μm and 479 μm). The difference in synaptonemal complex lengths in the male and female reported for zygotene (5), is also found at the pachytene stage. In the spermatocytes, the mean complement lengths amounted to 210 μm at early pachytene, 232 μm at mid and 213 μm at late pachytene (20).

3.2. Early diplotene

Early diplotene nuclei were similar to those in late pachytene, with respect to morphological features such as nuclear shape, centromere morphology and nucleolar structure. The centromeric chromatin was irregular in outline with electron dense parts around the synaptonemal complexes and the bipartite morphology of the secondary constrictions on bivalents 1, 9 and 16, typical for pachytene, could no longer be recognized. The major nucleoli in nuclei 28 and 29 were of type C, i.e. spherical and electron dense (Figure 7a), whereas nucleus 27 had a B type nucleolus.

The most advanced diplotene oocyte (no. 29) was larger and had mitochondria congregated in one half of the cell, in contrast to the cells at pachytene and the earliest stage of diplotene, where the mitochondria were located just outside the nuclear envelope.

The major characteristic of the four nuclei assigned to early diplotene is the ongoing elimi-

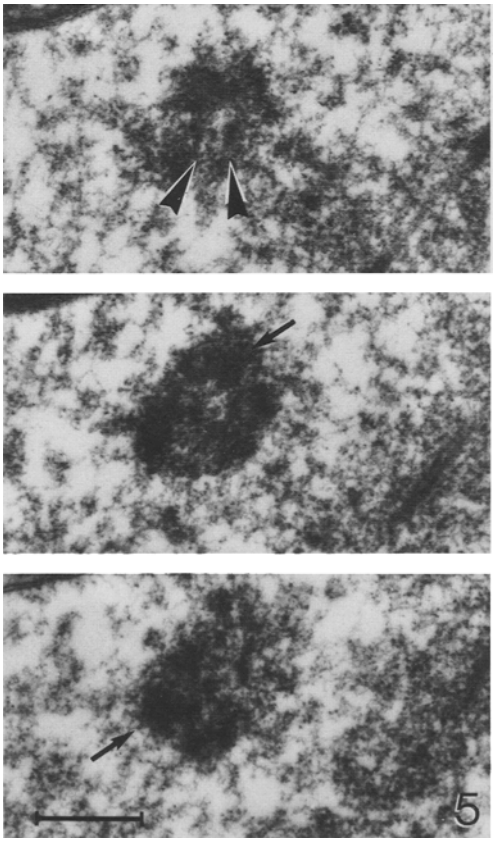

Figure 5. Three consecutive sections through a centromere region in a late pachytene nucleus. The electron dense chromatin areas are denoted by arrows. Arrowheads indicate the synaptonemal complex. (Bar = 0.5 μm).

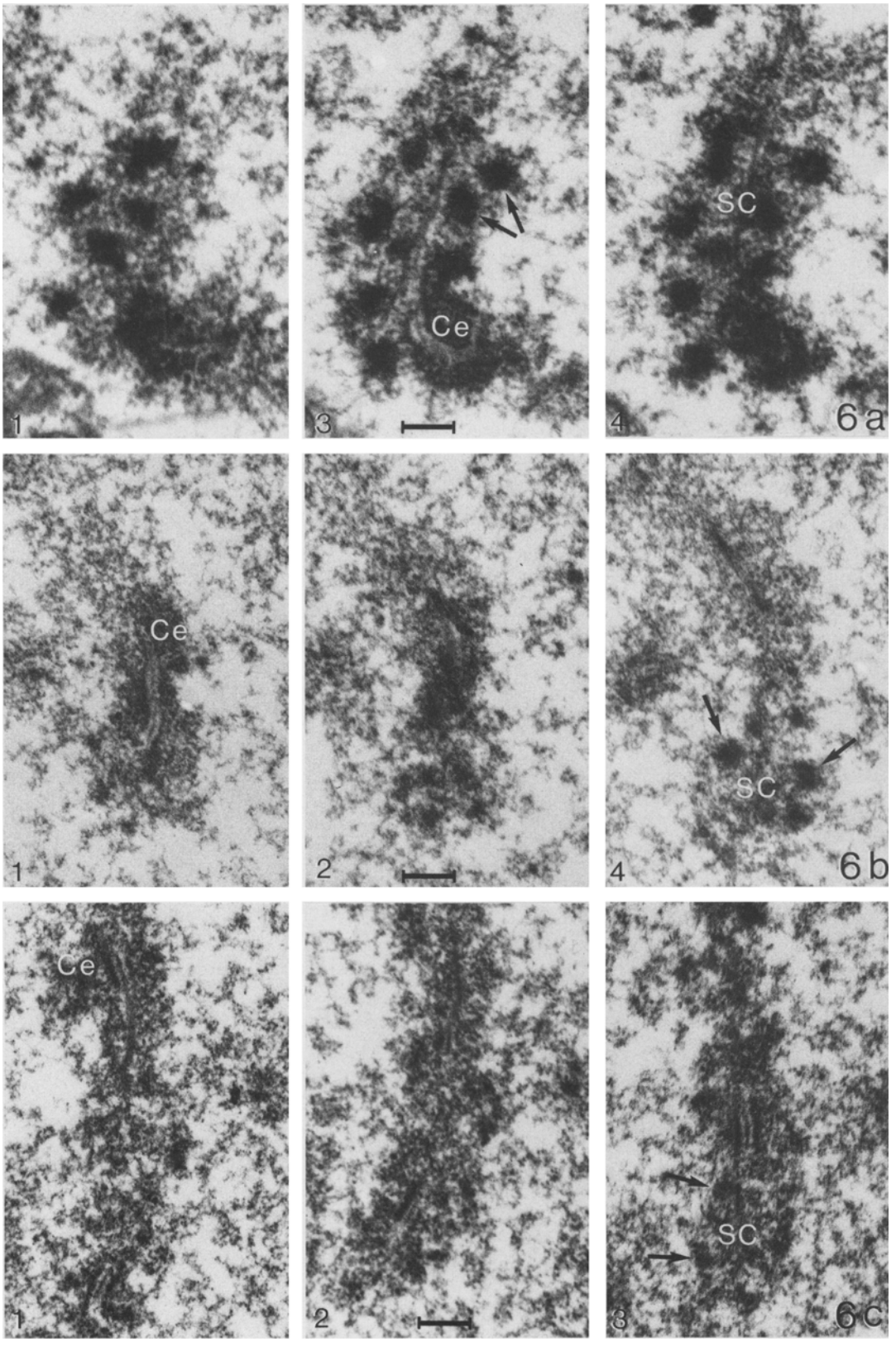
1
3
Ce
4
sc
6a
1
Ce
2
4
sc
6b
1
Ce
2
3
sc
6c

Figure 6. Electron micrographs showing the ultrastructure of the secondary constriction (SC) at early pachytene (Figure 6a), mid pachytene (Figure 6b) and late pachytene (6c). Arrows indicate the knobs. Ce, centromere. The numbers are the relative section numbers for the consecutive sections. (Bars = 0.5 μm).

nation of the synaptonemal complex. Structurally different kinds of degenerating complexes could be recognized. Most frequently, the central region was the first to disintegrate, so it no longer joined the lateral components. Homologous centromere regions were often separated, especially in the most advanced nucleus. The presence of paired and single lateral components is evident from the survey micrograph and the reconstructions in Figures 7a and 7b.

The total complement length was measured in one nucleus (no. 27) to be 442 μm, which is less than the mean of 519 μm measured at late pachytene, but within the limits of the complement lengths found at this stage.

One of the nuclei (no. 26), displayed only 5 μm of unpaired lateral components, which represents one percent of the complement. The breakdown of the synaptonemal complex was more advanced in the remaining three nuclei, which contained 52, 67 and 68 synaptonemal complex segments with combined lengths of 344

Table II.
Synaptonemal complex (SC) lengths and numbers of recombination nodules and bars in nuclei assigned to early, mid and late pachytene.

Stage	Nucleus number	SC length (μm)	Number of nodules	Number of bars	Total number of nodules and bars
	6	484	34	8	42
	7	601	68	4	72
Early	8	577	47	8	55
	9	518	50	15	65
pachytene	10	585	59	5	64
	11	566	48	9	57
	13	458	58	3	61
	14	431	61	0	61
	Mean ± sd	533 ± 72	53 ± 11	7 ± 5	60 ± 9
	12	415	49	10	59
Mid	15	451	46	18	64
	16	484	54	10	64
pachytene	17	453	45	13	58
	18	451	42	9	51
	19	496	49	9	58
	Mean ± sd	458 ± 29	48 ± 4	12 ± 4	59 ± 5
	20	646	38	13	51
	21	424	34	14	48
Late	22	456	33	14	47
	23	589	30	21	51
pachytene	24	525	18	22	40
	25	467	25	13	38
	26	524	27	21	48
	Mean ± sd	519 ± 78	29 ± 7	17 ± 4	46 ± 5

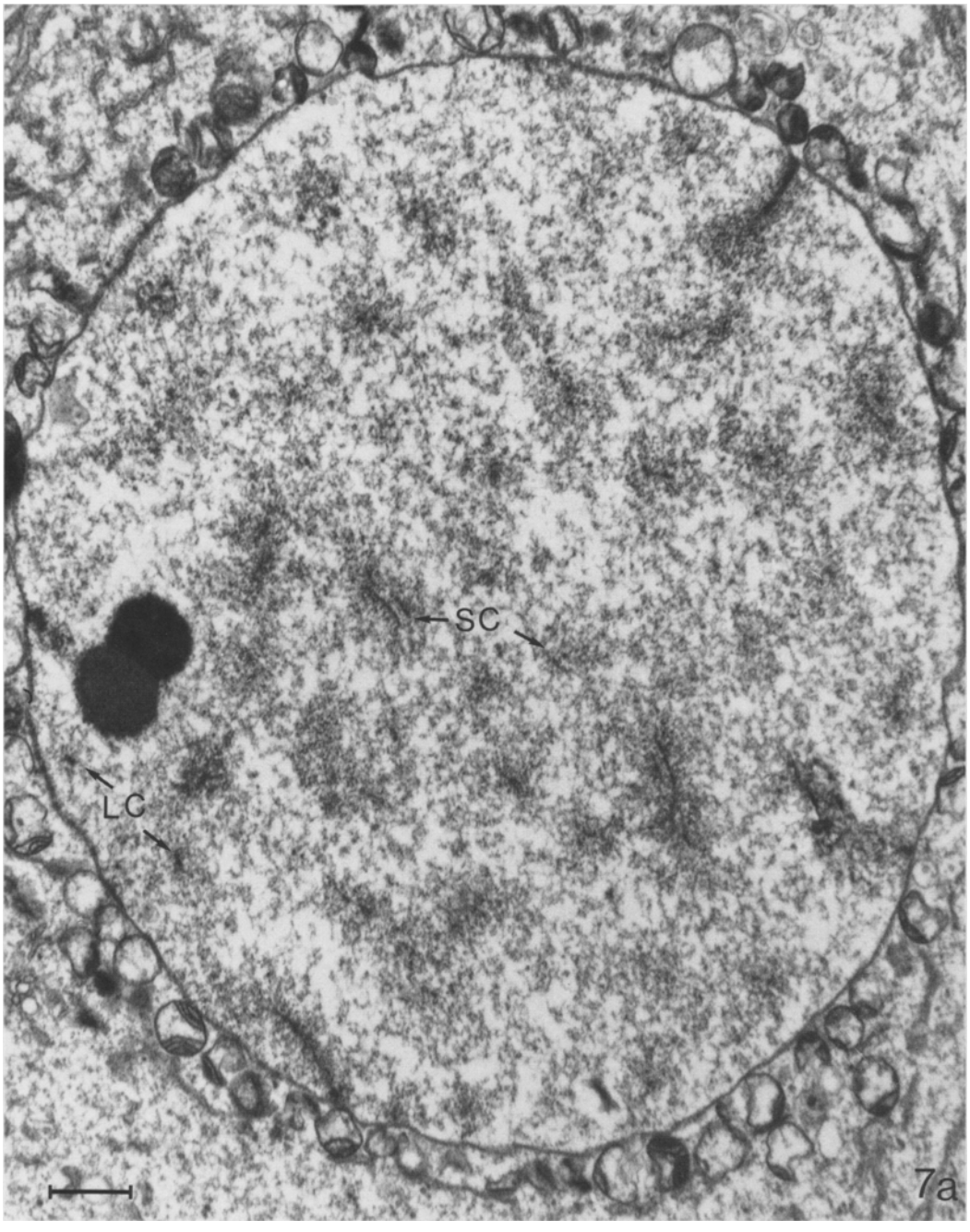

Figure 7a. Survey micrograph of an early diplotene nucleus. Several synaptonemal complexes (SC) and unpaired lateral components (LC) are seen in cross and longitudinal sections. (Bar = 1 μm).

μm, 234 μm and 90 μm (Table III). Thus, the reduction in length of the synaptonemal complex segments from 234 μm to 90 μm was not accompanied by any noticeable increase in the number of segments, the degradation of the central region of the complex apparently being

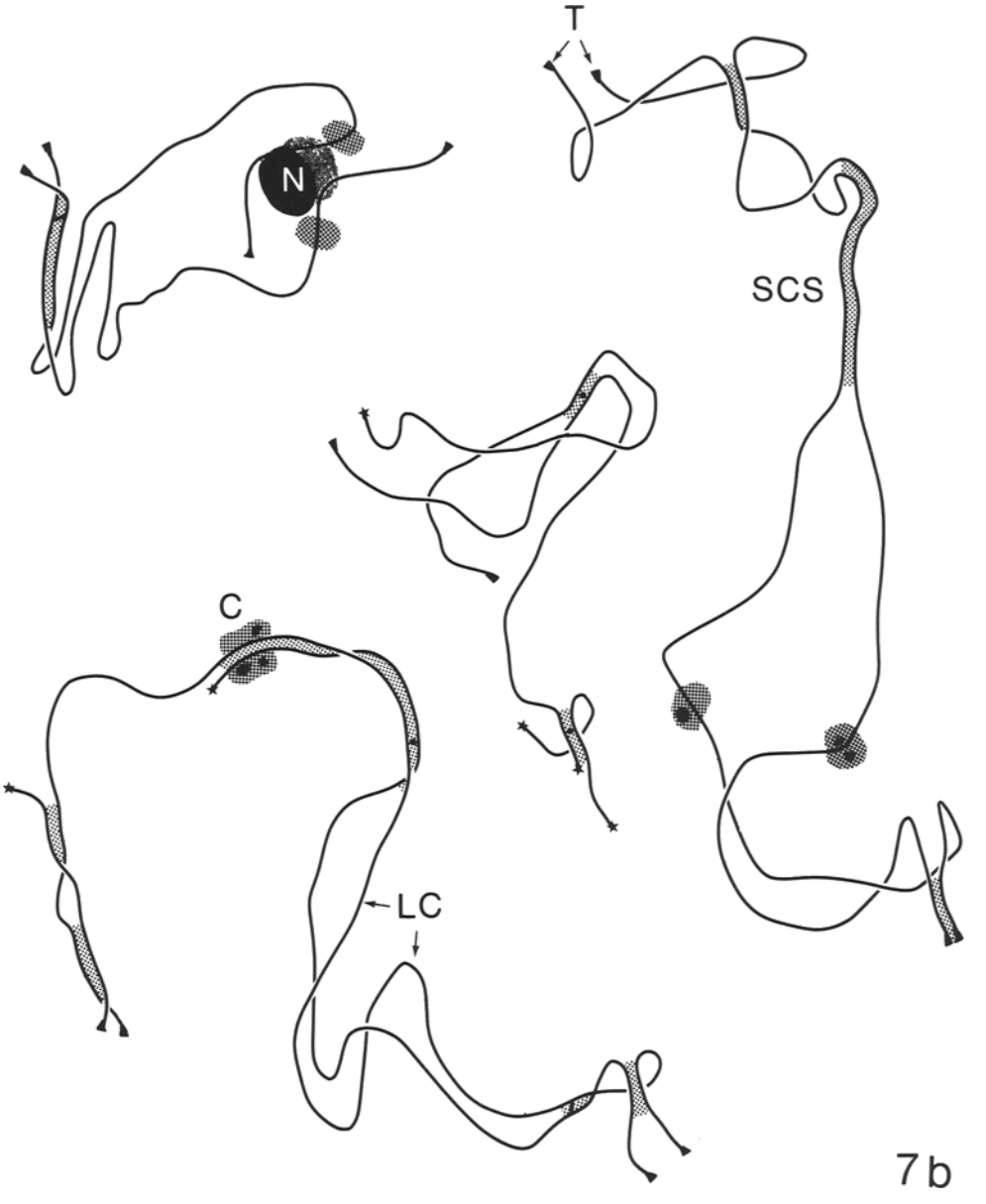

Figure 7b. Reconstructions of some early diplotene bivalents and bivalent fragments showing synaptonemal complex segments (SCS) and unpaired lateral components (LC). C, centromere regions; N, nucleolus; T, telomere attachment sites to the nuclear envelope. Asterisks denote discontinuous lateral components, recombination nodules are denoted by dots and bars are denoted by dashes.

initiated at a limited number of sites, whereafter the degradation proceeds from the ends of the segments.

The unpaired lateral components were frequently discontinuous, less frequently both lateral components and the central region were affected, resulting in bivalent discontinuities. Two bivalent and 16 chromosome discontinuities were observed in one nucleus (no. 27). As a consequence, assignment of synaptonemal

Table III.
Length and number of the synaptonemal complex segments (SCS) and number of recombination nodules and bars in the three early diplotene nuclei.

Nucleus number	SCS length (μm)	Number of SCS	Number of nodules	Number of bars	Total number of nodules and bars
27	344	52	23	19	42
28	234	67	15	15	30
29	90	68	13	6	19

complexes and lateral component segments to individual bivalents was not possible. In some cases only one of the lateral components and the central region had disintegrated, while the other lateral component was continuous (Figure 8). Degeneration of the synaptonemal complexes occurred also at the telomeres, and of the 92 attached telomeres seen at pachytene, only 90, 86 and 65 were attached to the nuclear envelope in nuclei 27, 28 and 29, respectively. In some cases, the lateral components were split longitudinally in the vicinity of the attachment site.

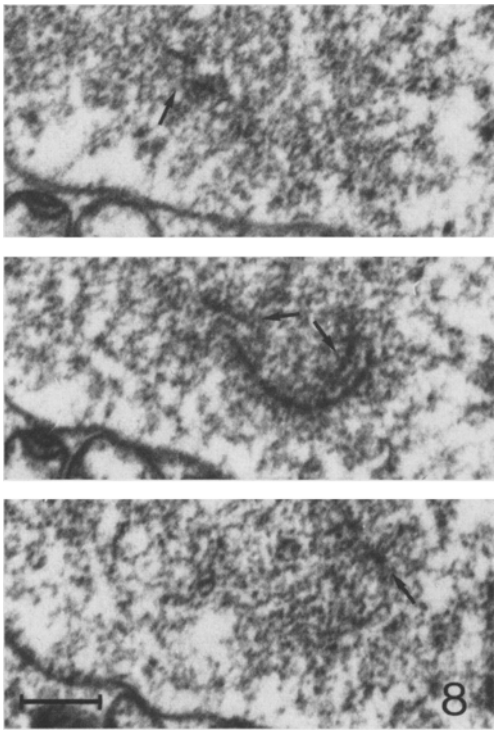

Figure 8. Three sections through an early diplotene bivalent with degenerating synaptonemal complex. One of the lateral components and the central region are discontinuous. The segment of degenerating synaptonemal complex is flanked by intact synaptonemal complex segments (arrows). (Bar = 0.5 μm).

In contrast to the situation in the spermatocytes, where virtually all recombination nodules and bars have disappeared by late pachytene, nodules and bars were still present within some intact segments in the diplotene oocytes. Their number, together with the length of synaptonemal complexes and the number of synaptonemal complex segments in the three nuclei, are given in Table III.

3.3. Mid diplotene

Oocytes at the mid diplotene stage are easily distinguishable as primordial follicles, being partially or totally surrounded by flattened granulosa cells. Moreover, the oocytes are larger and more spherical than at earlier stages. The mean diameter of the three analyzed nuclei was 17.2 ± 2.2 μm, compared to 12.4 ± 2.4 μm of pachytene nuclei. The mitochondria, which during zygotene and pachytene surrounded the nuclear envelope, have congregated into one half of the cell (compare Figures 7a and 9).

The three serially sectioned nuclei revealed one to three large, irregular nucleoli consisting of a reticulum of electron dense material with more or less electron transparent cavities. In Figure 9, a spherical core of medium electron density is present within the network.

The chromatin was evenly dispersed throughout the nucleus and only slightly condensed around the lateral components of the synaptonemal complex, which appeared as single, elec-

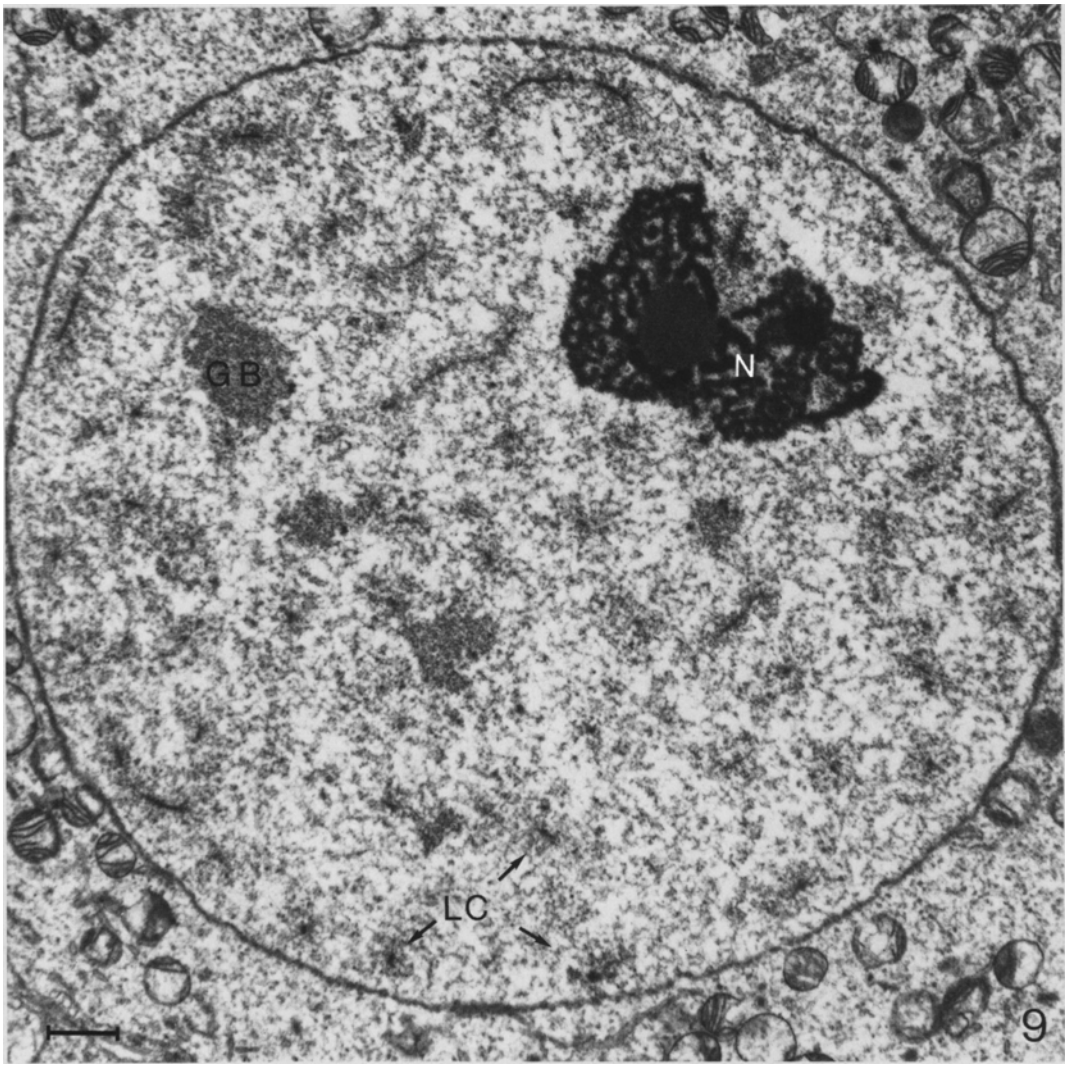

Figure 9. Survey micrograph of a mid diplotene nucleus. Single lateral components (LC) are seen in cross and longitudinal sections. In the nucleolus (N), spherical cores of high and medium electron density are present. Note that mitochondria no longer encompass the nuclear envelope. GB, granular bodies. (Bar = 1 μm).

tron dense threads, approximately 60 nm in diameter.

A reconstruction of the remnants of the synaptonemal complexes in one mid diplotene nuclei was attempted. Although most of the lateral components could only be traced over few sections, some were continuous over longer distances, perhaps over their entire length. All lateral component stretches ended in the nucleoplasm or in the vicinity of irregular, granulo-fibrillar bodies containing electron dense knobs (Figure 9). The telomeric regions could thus no longer be recognized either by attachment to the membrane, or by the conical thickening of the lateral components, characteristic of the earlier stages.

The centromeres appeared as electron dense spheres with a diameter of 350 nm (Figure 11a). Sixteen of the 46 centromeric regions were joined in pairs, probably consisting of homolo-

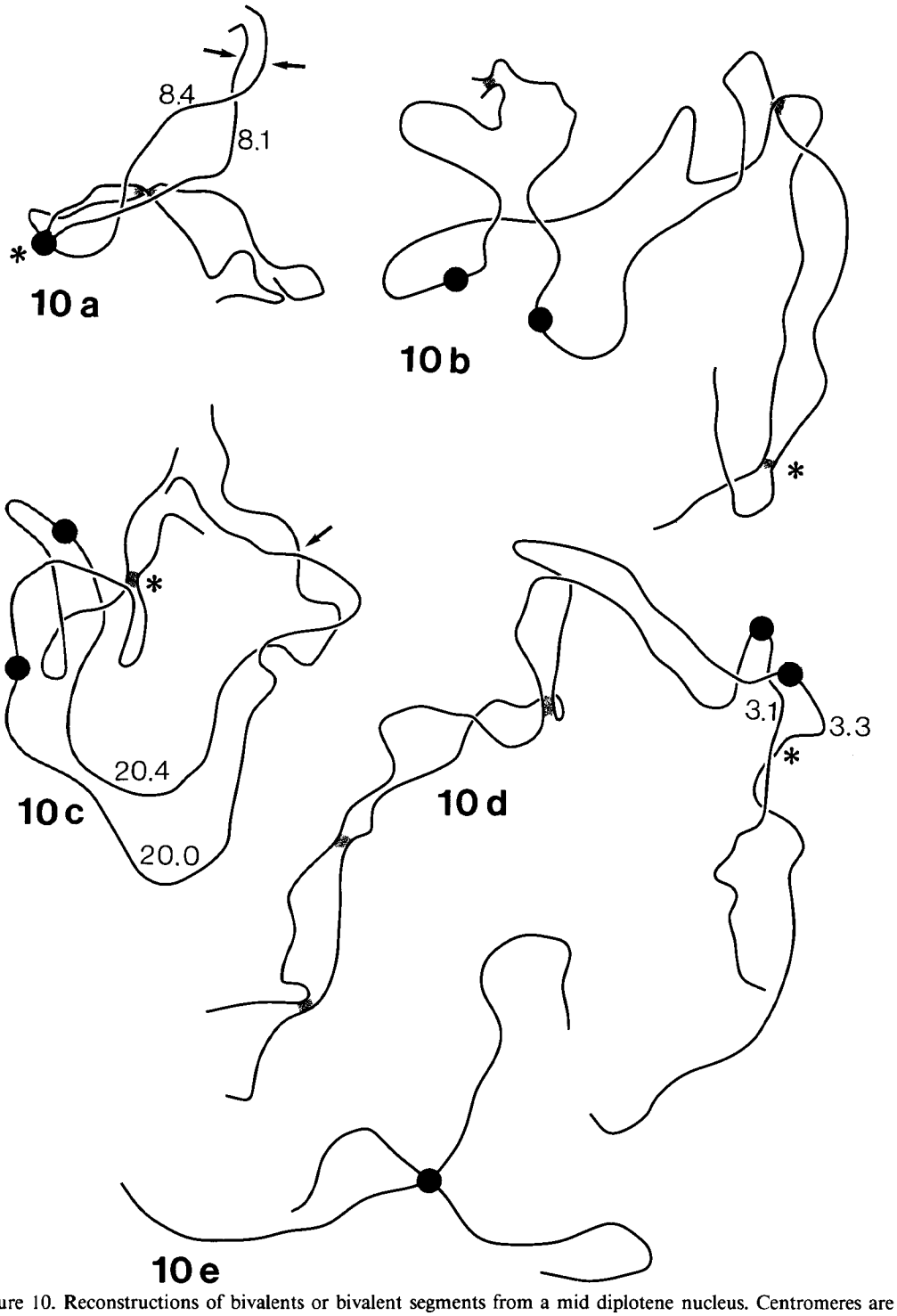

Figure 10. Reconstructions of bivalents or bivalent segments from a mid diplotene nucleus. Centromeres are shown in black, segments paired with synaptonemal complexes are denoted by light hatching. The numbers indicate the distances in μm, from the centromeres to the points where the spacing of the lateral components of unpaired homologous chromosomes are less than or equal to 0.5 μm (arrows). The regions denoted by asterisks are shown in electron micrographs in Figure 11.

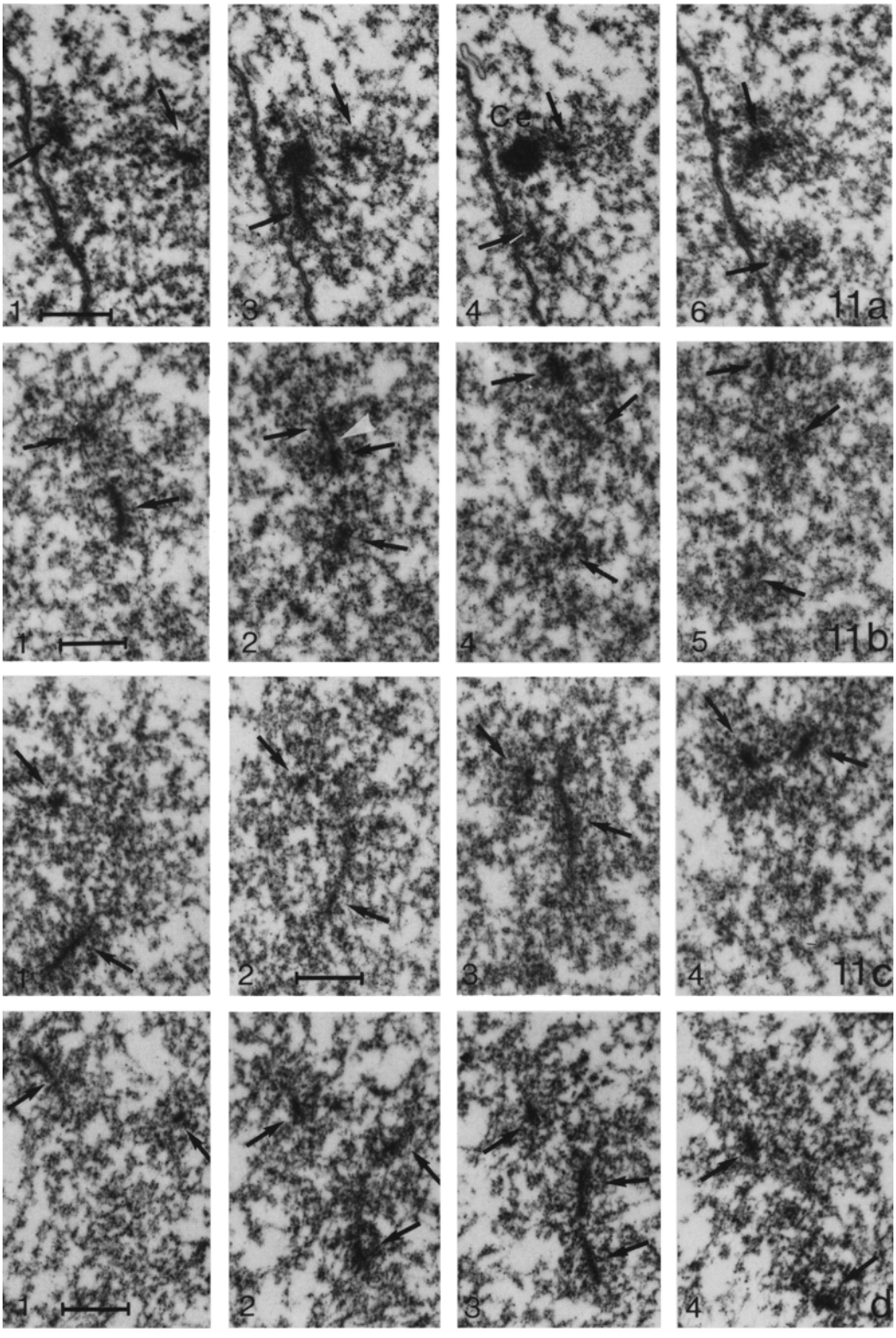
1
3
4
6
11a
1
2
4
5
11b
1
2
3
4
11c
1
2
3
4
d

Figure 11. Electron micrographs of sections through the regions denoted by asterisks in Figure 10. The numbers are the relative section numbers for the consecutive sections. (Bars = 0.5 μm). Figure 11a. Series of sections through the confluent centromere regions (Ce) of two homologous chromosomes (lateral components are denoted by arrows) (see Figure 10a). Figure 11b. Sections through a presumptive chiasmata. The two homologous lateral components (arrows) are connected at a single point by a remnant of the central region of the synaptonemal complex (white arrowhead) (see also Figure 10b). Figure 11c. Four consecutive sections through two homologous lateral components (arrows) connected by a retained central region of the synaptonemal complex. Note, in the retained segment, a structure resembling a dissolving recombination bar. (see also Figure 10c). Figure 11d. A series of consecutive sections through two homologous lateral components (arrows) aligned at a distance of 0.5 μm. The chromosomes are widely separated over the rest of their lengths. Note that no remnants of the central region of the synaptonemal complex or other structures can be recognized between the two homologues in the region of alignment (see also Figure 10d).

gous centromeres. Figures 10a and 10e are reconstructions of two such bivalents or bivalent fragments, and Figure 11a is a series of micrographs through the confluent centromere regions of two homologues.

The chromosomes in Figure 10a are not only joined at the centromeres, but are also paired by one short stretch of synaptonemal complex. Similar synaptonemal complex segments joining other pairs of chromosomes are shown in Figures 10a-d. The segments are only 0.1-0.2 μm long and therefore difficult to detect unless reconstruction is performed. The short arm of the bivalent shown in Figure 10b has one, and the long arm two paired regions. The distal region is shown in a series of micrographs in Figure 11b. In five cases, structures probably representing dissolving recombination bars were observed in the paired region. One example is shown in Figure 11c, which is a series of micrographs of the region denoted by an asterisk in Figure 10c.

Of the 39 regions paired with a short segment of synaptonemal complex, 18 were between homologous chromosomes as evidenced by the similarity of the lateral component lengths between the centromeres and the synaptonemal complex segments. In the remaining 21 cases, the lateral components flanking the paired regions were too short to allow a determination of homology. On the other hand, association was never observed between decidedly nonhomologous chromosomes. No other structures were observed to join the homologues and thus it is conceivable that these paired regions represent early chiasmata.

Most of the reconstructed bivalents possessed such presumptive chiasmata, although some bivalents and bivalent arms, such as those shown in Figures 10a and 10c-10e, were devoid of synaptonemal complexes. Reconstructions of the lateral components of such bivalents revealed a total of seven positions where the otherwise widely separated two lateral components approached each other to a distance of only two to three times the width of the central region. Remnants of the central region or derivatives hereof could, however, not be recognized at these sites.

Figure 10d is a reconstruction of two chromosomes, in which the long arms are joined at three positions by segments of the synaptonemal complex. The short arms are widely separated, except at one point where the distance between them is 0.5 μm. Figure 11d is a series of micrographs through this association point. The distances from this point to the respective centromeres were measured to be 3.3 μm and 3.1 μm (Figure 10d). Reconstructed bivalents in Figures 10a and 10c present other examples of homologous chromosome arms held together at distances of about 0.5 μm. The distances from the centromeres to the presumptive chiasmata were virtually identical for the two homologous chromosome arms, amounting to 8.1 μm and 8.4 μm (Figure 10a), and 20.4 μm and 20.0 μm (Figure 10c), respectively.

This equality in length strongly suggests that the observed associations are chiasmata, and furthermore indicates that in the human female the synaptonemal complex does not persist beyond diplotene, but that, in the course of

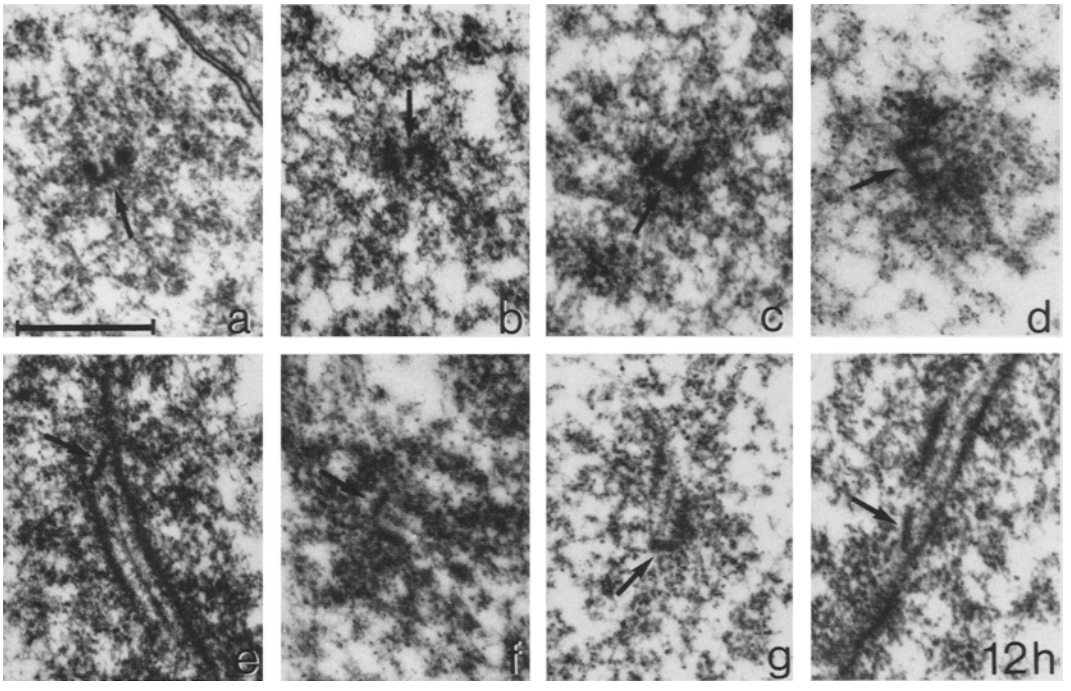

Figure 12. Electron micrographs showing intermediates betwen recombination nodules and bars (Figures 12a-c) and recombination bars (Figures 12d-h). The structures are denoted by arrows. Figures 12c and f are both oblique sections. (Bar = 0.5 μm).

diplotene, the remnants of the central region dissolve leaving the chiasmata without recognizable derivatives of the synaptonemal complex. This conclusion is supported by preliminary investigations of diplotene nuclei from adult women. In these nuclei no traces of central regions can be recognized.

3.4. Recombination nodules and bars

As described previously (5), recombination nodules that attach to the central region of the synaptonemal complex at zygotene are spherical to oblong, some of them developing prominent connections to the lateral components of the complex (Figures 12a-c). During pachytene some of the nodules change in appearance. The spherical part can no longer be recognized and the structure consists of an electron dense bar bridging the central region of the synaptonemal complex at a right or an oblique angle (Figures 12d-h).

Table IV gives the mean numbers of recombination nodules and bars in oocytes and spermatocytes at late zygotene, early, mid and late pachytene and early diplotene.

In the oocytes, during the period from late zygotene to late pachytene, the total number of recombination structures decreases gradually from a mean of 68 to 46 per nucleus. This decrease is due to a reduction in the number of recombination nodules, whereas the mean number of recombination bars increases from 6 to 17.

In the spermatocytes, a much more drastic reduction of recombination structures, from a mean of 101 to 10, is observed over the same period. Moreover, the number of recombination nodules decreases from 68 to 9 from early to mid pachytene, while the number of bars increases from 6 to 32 per nucleus. Thus at mid pachytene, recombination bars dominate in the spermatocytes, while in the oocytes nodules are more frequent than bars at all stages.

Table IV.
Mean numbers of recombination nodules and recombination bars in late zygotene, early, mid and late pachytene and early diplotene nuclei of human oocytes and spermatocytes. O, oocytes,: S, spermatocytes,: sd, standard deviation.

Stage	n		Number of recombination nodules (±sd)		Number of recombination bars (±sd)		Total number of recombination structures (±sd)	
	O	S[1]	O	S[1]	O	S[1]	O	S[1]
Late zygotene[2]	5	10	63±11	101±25	6±3	0	68±10	101±25
Early pachytene	8	33	53±11	68±20	7±5	6±9	60±9	74±18
Mid pachytene	6	29	48±4	9±5	12±4	32±8	59±5	41±9
Late pachytene	7	11	29±7	3±2	17±4	7±7	46±5	10±8
Early diplotene	3	2	17±5	0	13±7	0	30±11	0

[1] Data from HOLM and RASMUSSEN, (20, 21, 27)
[2] The sample of spermatocytes have 72% of the chromosome complement paired with a synaptonemal complex, whereas the oocytes display 98% pairing.

In the three early diplotene oocytes the mean number of recombination structures is reduced to 30, the reduction affecting both recombination nodules and bars. A further reduction accompanies the elimination of the synaptonemal complex, and by mid diplotene the recombination nodules are only occasionally observed. Thus in oocytes, the recombination nodules and bars persist longer than in spermatocytes, where virtually all recombination structures are eliminated by the end of pachytene (20).

3.5. Distribution of recombination nodules and bars among the bivalents

Upon analysis of the number and distribution of recombination nodules and bars in human spermatocytes, it was concluded that while a nodule represents a potential for crossing over, the morphological change from nodule to bar signifies the actual occurrence of crossing over (20).

In order to examine whether nodules and bars were distributed at random among the bivalents and bivalent arms and whether their distribution changed in the course of meiotic prophase, the observed distributions were compared to those expected if the structures were positioned at random. As the distribution pattern of recombination nodules and bars seemed very similar, the data for both structures are pooled in the following way. The random distributions were obtained with the aid of a Honeywell Bull H 6000 computer fed with absolute lengths and centromere indices of all bivalents together with the number of nodules and bars of the individual nuclei. The computer was programmed to position individual recombination structures at random, one at a time, and no closer than 80 nm from a previously positioned nodule or bar and no closer than 40 nm from a telomere or a centromere. The program was run 10,000 times for each stage, the number of runs for a given nucleus corresponding to 10,000 divided by the number of nuclei reconstructed for that stage. In this way, the random frequencies of bivalents and bivalent arms with 0, 1, 2, 3, 4, 5 and $\geqslant$ 6 nodules and bars were obtained.

As seen in Tables V and VI, at zygotene and early pachytene, the observed frequencies of bivalents and bivalent arms with one or more

Table V.
Distribution of recombination nodules, bars and chiasmata among the bivalents in human oocytes. O, observed frequencies, E, frequencies expected upon random distribution of nodules and bars among bivalents.

Stage		Percent bivalents with n nodules and bars or chiasmata						
	n=	0	1	2	3	4	5	⩾6
Late zygotene	O	3	18	21	22	20	8	7
	E	9	18	20	18	13	9	13
Early pachytene	O	8	21	24	20	14	9	5
	E	12	21	22	18	12	7	8
Mid pachytene	O	4	23	26	20	12	9	3
	E	11	21	23	18	12	7	7
Late pachytene	O	8	28	33	21	10	0	0
	E	17	27	24	16	16	0	0
Diakinesis[1]	O	[2]	41	39	13	5	2	0

[1] n equals the number of chiasmata, data from JAGIELLO et al.(24)
[2] a pair of univalents was observed in two cells

recombination structures are virtually identical to the frequencies obtained by random positioning of nodules and bars. At mid and late pachytene, however, more bivalents and bivalent arms possessed a nodule/bar than can be accounted for by random distribution. Especially, frequencies of bivalents with two and bivalent arms with one nodule/bar exceed the expected ones.

At all stages a marked deviation from randomness is apparent for bivalents devoid of recombination structures. Only two-thirds of the expected number of bivalents without recombination structures were observed at early pachytene, one-third at late zygotene and mid pachytene stages and one-half at late pachytene. Also the frequency of bivalent arms without nodules is lower than expected, although the difference between the observed and expected

Table VI.
Distribution of recombination nodules and bars among the bivalent arms in human oocytes. O, observed frequencies, E, frequencies expected upon random distribution of nodules and bars among bivalents.

Stage		Percent bivalent arms with n nodules and bars						
	n=	0	1	2	3	4	5	⩾6
Late zygotene	O	26	30	24	12	5	2	1
	E	30	29	20	11	6	3	1
Early pachytene	O	33	29	21	11	5	1	0
	E	34	30	19	10	5	3	0
Mid pachytene	O	27	37	22	9	4	1	0
	E	34	30	19	10	4	2	0
Late pachytene	O	34	39	21	6	1	0	0
	E	42	31	17	7	3	0	0

Figure 13. Distribution of distances between telomeres and the most distal recombination nodule or bar (left column) and distance distribution for neighbour nodules/bars (right column) at late zygotene and early, mid and late pachytene. The histograms show the distribution of the observed distances expressed for each distance class as the mean of that particular class and the two classes on either side. The dots represent the relative frequencies of distances expected, if nodules and bars were distributed at random. Abscissa, number of 0.1 μm distance classes. Ordinate, relative frequency of distances.

values is not as pronounced as when entire bivalents are considered.

Table V also includes frequencies of bivalents with 1, 2, 3, 4 and 5 chiasmata, which are calculated from data reported by JAGIELLO et al. (24), who counted the number of chiasmata in 621 diakinesis bivalents in oocytes matured in vitro. The frequency of bivalents with one or two chiasmata is higher than the frequency of bivalents with one or two nodules, whereas the opposite is the case for bivalents with three or more chiasmata.

3.6. Neighbour nodule/bar and telomere - nodule/bar distributions

Inspection of reconstructed bivalents reveals that nodules and bars are more frequent in the vicinity of the telomeres than at other positions along the bivalent arms. The frequencies of observed distances between telomeres and the closest recombination structures were compared to the random frequencies of distances obtained by the computer simulation described previously. From Figure 13 it is evident that at all stages the observed frequencies deviate from the expected ones. More nodules/bars than expected are present in the distal 1.5 μm of the bivalents, except for the most distal 0.1-0.3 μm, where less nodules are observed.

As described in section 3.4, the number of recombination structures gradually decreases from a mean of 68 per nucleus at late zygotene to a mean of 30 at early diplotene. Despite this elimination, the frequency of bivalents and bivalent arms without recombination structures does not increase and the non random distribution of nodules and bars among the bivalents is retained. In order to further investigate this elimination process, neighbour nodule/bar distances were compared to the distance distribution obtained by random positioning of recombination structures at the different substages. As seen in Figure 13, at late zygotene and early pachytene, the major deviation from the random frequencies is an excess of distances of about 1 μm and a corresponding deficit of longer distances. At later stages, differences between the two distributions become more prominent. At mid pachytene, the distances of about 1 μm are only slightly more common than expected. Hence the removal of recombination structures is differential and affects primarily nodules and bars located close to others. Moreover, a pattern of peaks and troughs in the distance distribution is evident at mid pachytene. This pattern is even more pronounced at late pachytene when neighbour nodule/bar distances of 1.5, 3.0, 6.0, 7.5 and 12 μm are especially frequent.

3.7. Distribution of nodules and bars along bivalents

The observations described in the last section suggest that the nodules and bars are unevenly distributed along the arms and tend to be spaced at particular distances. The distribution of nodules and bars along the individual bivalents was therefore investigated.

Twelve of the 23 bivalents in the prophase oocytes, i.e. bivalents 1-3, 6, 9, and 16-22, can be identified on the basis of length, centromere index and structural markers. For the remaining eleven bivalents, an assignment beyond groups B, C and D is more uncertain (5).

Corresponding bivalent arms from all reconstructed nuclei were normalized to their mean length maintaining the relative positions of nodules and bars. Each arm was then divided into the same number of intervals as that used when the corresponding bivalent arm in spermatocytes (20) was divided into 0.67 μm intervals. This was done in order to facilitate the comparison of nodule and bar distributions in the two

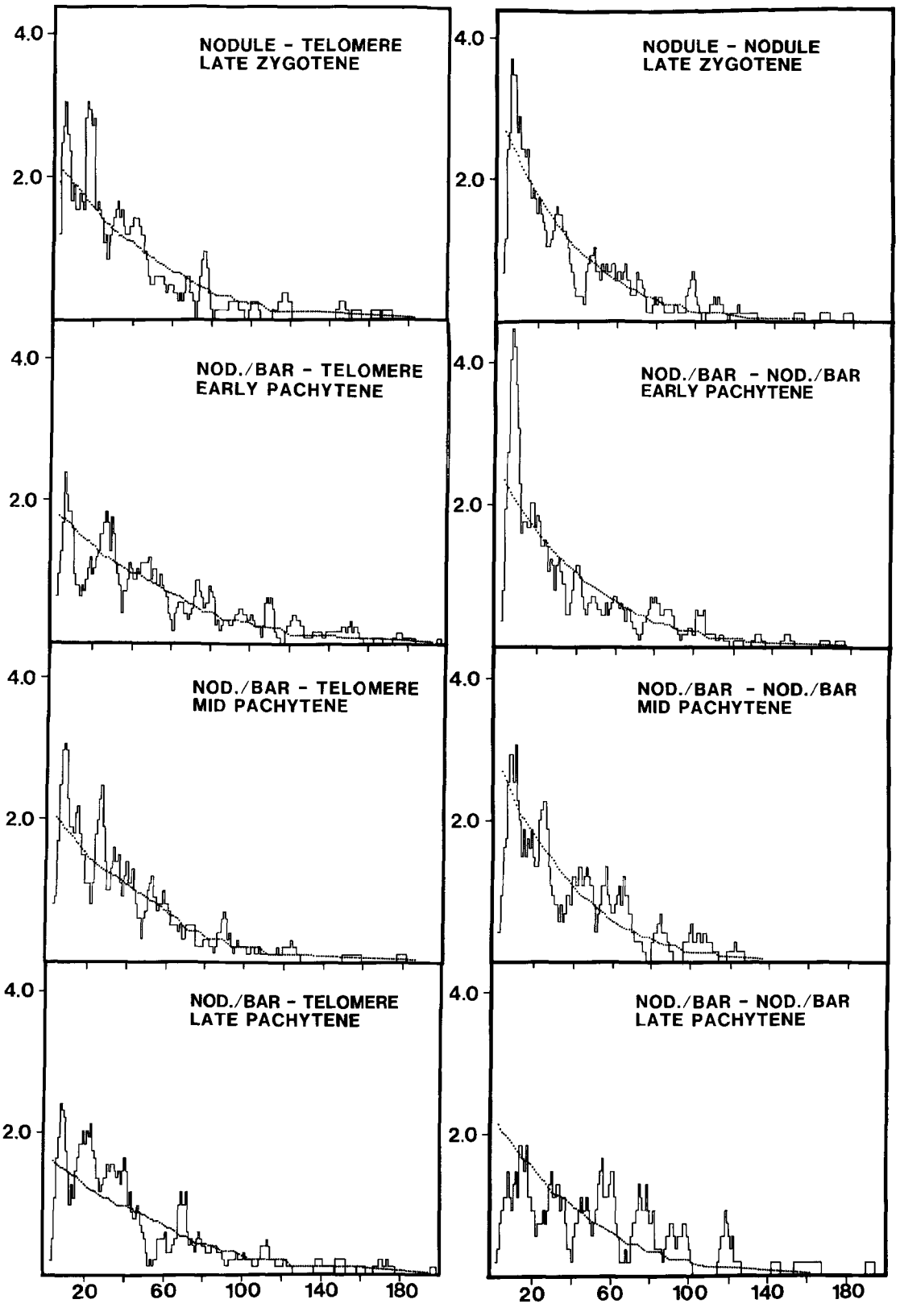
NODULE - TELOMERE
LATE ZYGOTENE
NODULE - NODULE
LATE ZYGOTENE
NOD./BAR - TELOMERE
EARLY PACHYTENE
NOD./BAR - NOD./BAR
EARLY PACHYTENE
NOD./BAR - TELOMERE
MID PACHYTENE
NOD./BAR - NOD./BAR
MID PACHYTENE
NOD./BAR - TELOMERE
LATE PACHYTENE
NOD./BAR - NOD./BAR
LATE PACHYTENE
4.0
2.0
20
60
100
140
180

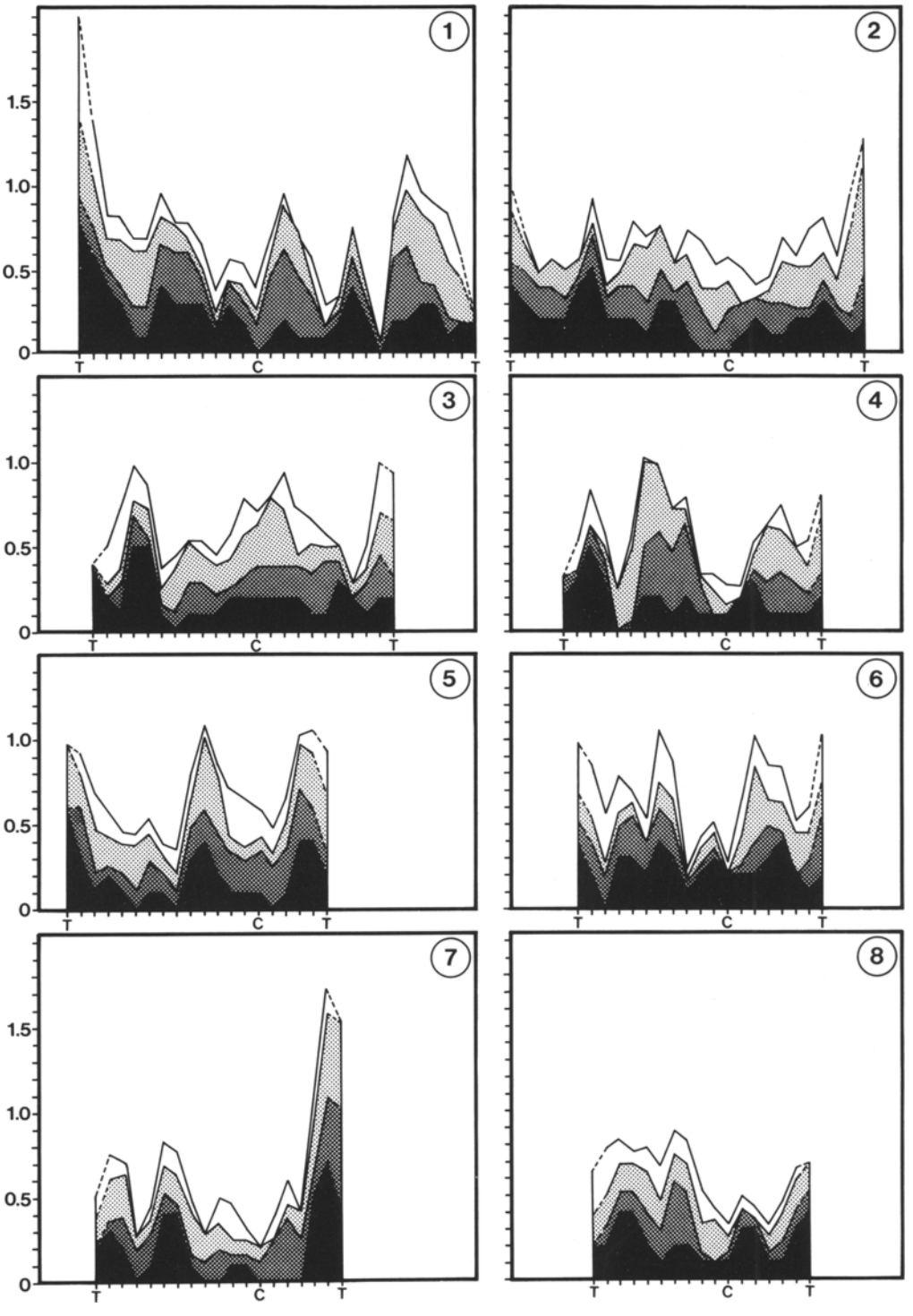

Figure 14. Cumulative distribution of recombination nodules and bars along the bivalents at late zygotene (black area), early pachytene (dark hatching), mid pachytene (light hatching) and late pachytene (no hatching). Abscissa, the normalized length of bivalents, T and C indicating the positions of telomeres and centromeres

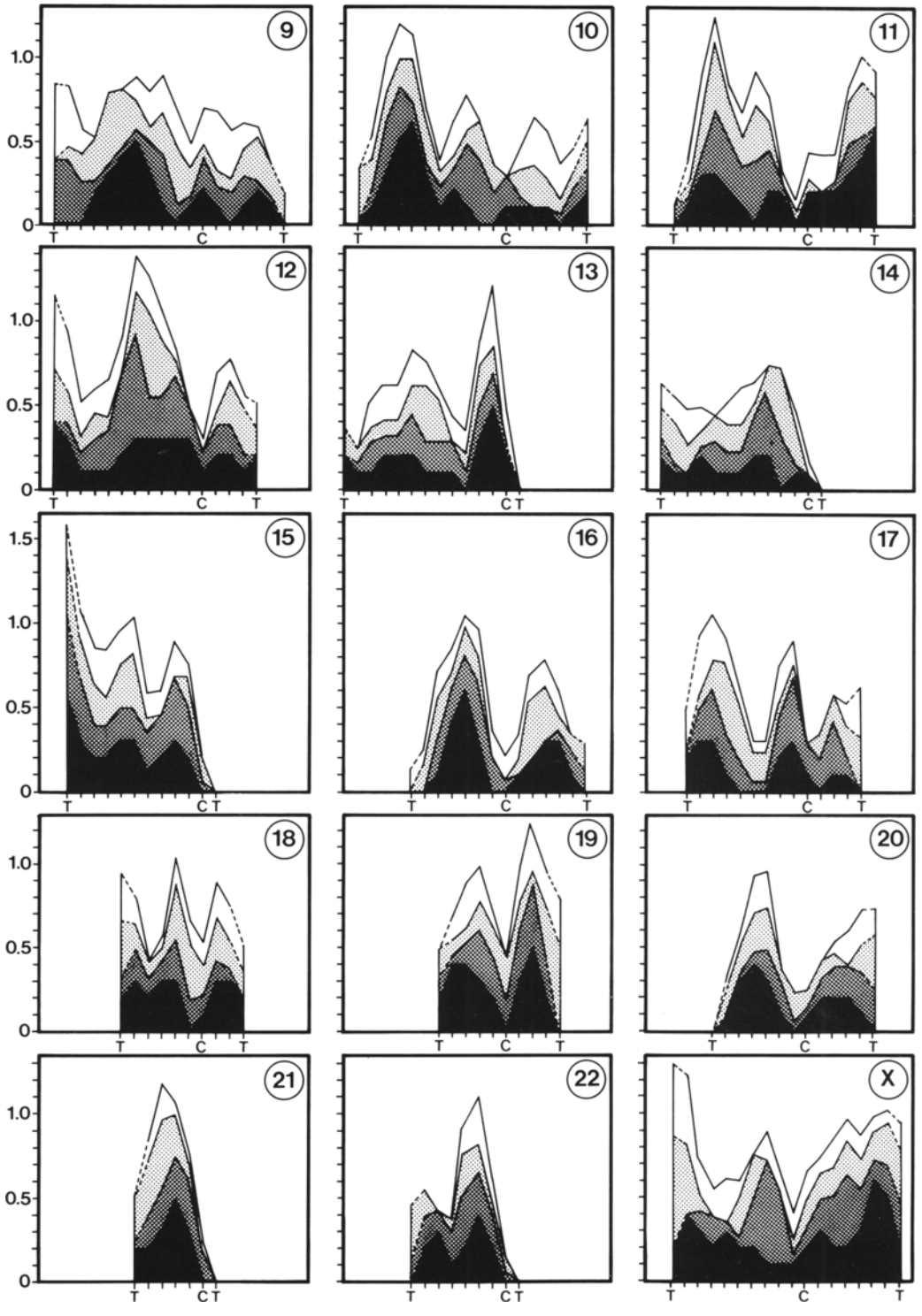

respectively. Ordinate, the number of nodules per nucleus per interval. The frequencies plotted in the diagram are the means of two adjacent intervals, except for the telomeric segments which are represented by their actual nodule frequencies.

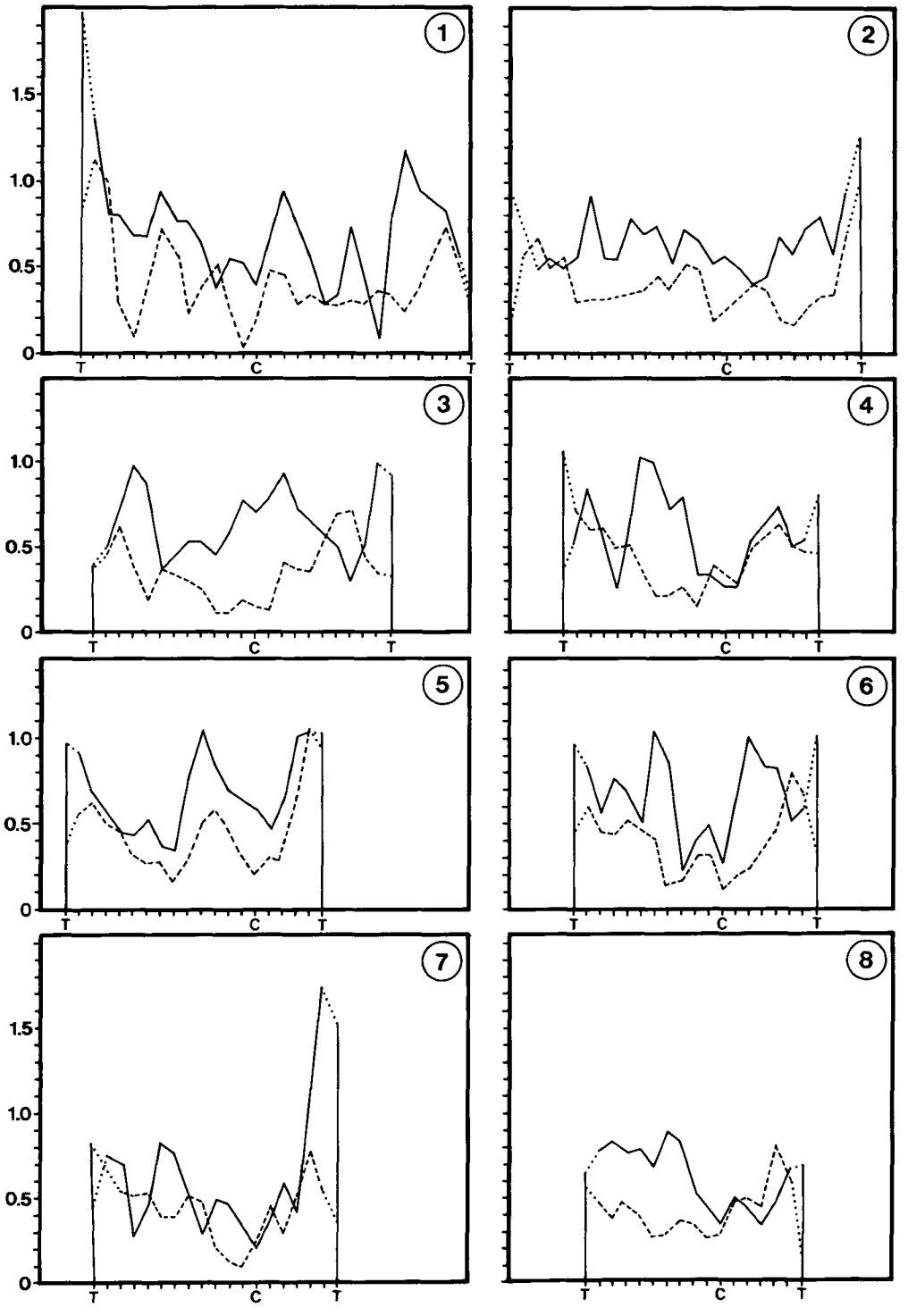

Figure 15. A comparison between the cumulated distributions of recombination nodules and bars from late zygotene to late pachytene in oocytes (solid line) and from early to late pachytene in spermatocytes (dashes) for the 22 autosomal bivalents. The data for the spermatocytes are from HOLM and RASMUSSEN (20). See also legend to Figure 14.

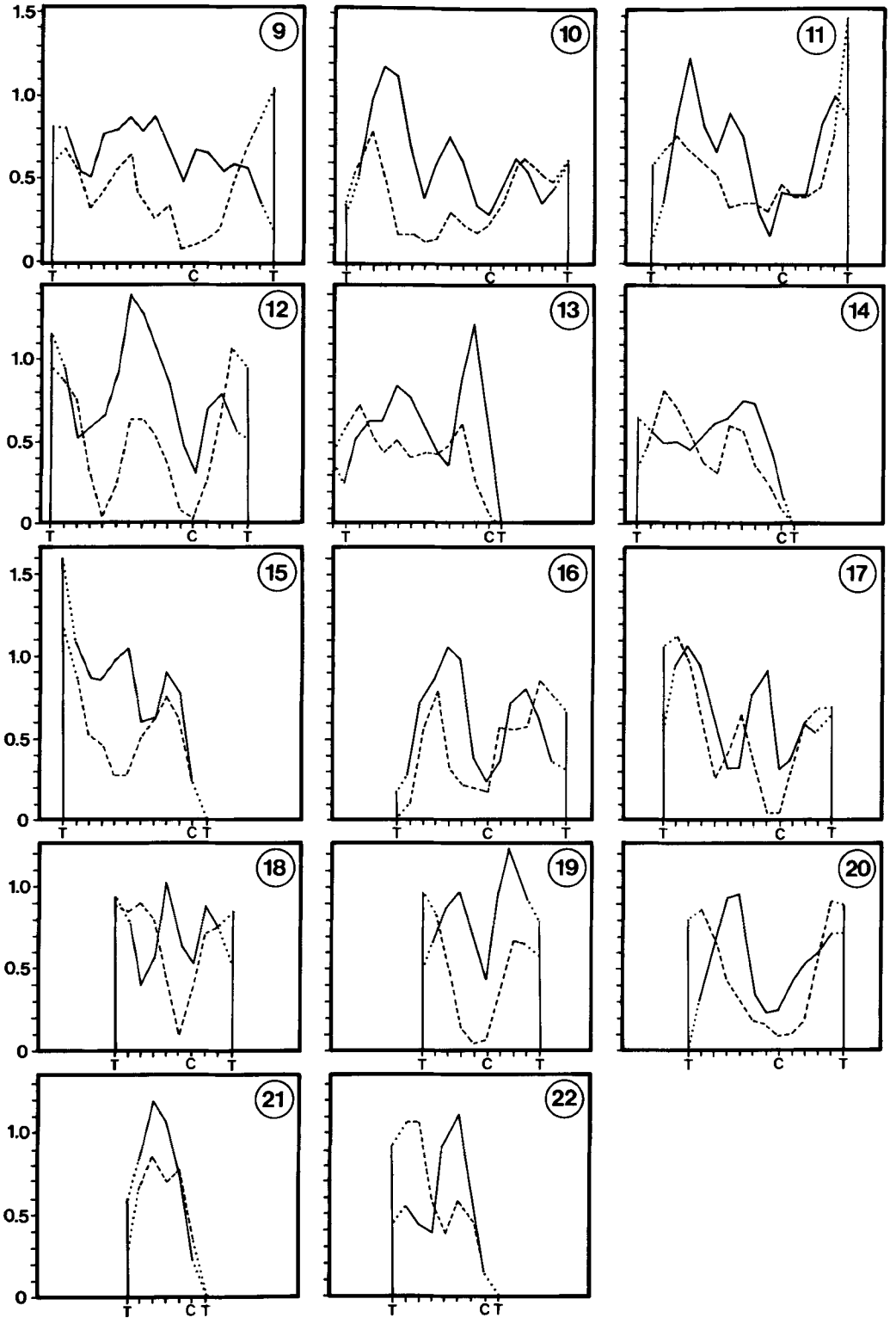
9
10
11
12
13
14
15
16
17
18
19
20
21
22
1.5
1.0
0.5
0
T
C
T

sexes which differ on an average by a factor of 2 in bivalent length. As a consequence, in the oocytes, the interval lengths used for the individual bivalent arms ranged from 1.20 μm to 1.62 μm. This gives a mean interval length of 1.41 μm and a standard deviation of 0.1 μm. The X bivalent, which did not have its counterpart in the spermatocytes was thus divided into 1.41 μm intervals.

The distributions of nodules and bars at late zygotene and in successive pachytene stages were cumulated. The frequency of recombination structures in a given interval, at a given stage was added to that of the preceeding stage or stages. In Figure 14, the contributions from early, mid and late pachytene are one by one added to the zygotene distribution.

The following features are apparent from the distributions presented in Figure 14.

1) Nodules and bars are distributed along the bivalents in a nonrandom manner; regions with high frequency of recombination structures alternate with regions with low frequency.

2) The pattern established at zygotene is retained during the following stages, as the contributions from the early, mid and late pachytene stages gradually enhance the peaks and do not eliminate the troughs along the bivalents.

3) The number of regions with a high frequency of nodules and bars in a bivalent arm correlates with the arm length. One often medial peak is present in the shortest arms such as the short arm of bivalents 12, 16, 18-20 and the long arms of bivalents 16, 19-21. Arms of intermediate length have either two distinct peaks (the short arms of bivalents 3, 4, 6, 8 and 10 and the long arms of bivalents 10-12 and 17-18), or, as seen in the long arms of bivalents 3-5 and 13-14, the two peaks have one to two shoulders. The longest arms (both arms of bivalent 1 and the long arm of bivalent 2) have 3 or 4 peaks. In agreement with the earlier observation that nodules appear with high frequency in telomeric regions, major peaks are seen in terminal to subterminal regions.

4) Recombination structures are virtually never observed in the short arms of the acrocentric chromosomes and, in most bivalents, there is a conspicuous trough in the vicinity of the centromere.

A comparison of the nodule/bar distributions in human oocytes and spermatocytes is shown in Figure 15. The distribution in the spermatocytes was obtained by adding the distribution of bars at early pachytene to the distribution of nodules and bars at mid and late pachytene (20).

From Figure 15 it is apparent that distribution of recombination structures along the bivalents is very similar in the two sexes. The distribution along bivalents 5, 8, 10, 12, 14, 16, 17, 19, 20 and 21 is the same, bivalents 1, 6, 7, 9, 11, 13, 15, 18 and 22 have very similar relative distributions, and pronounced differences are only seen in bivalents 2, 3 and 4.

Thus, it is apparent that despite the twofold longer bivalent complement in the female, the distribution of crossovers along the bivalents is very similar in the two sexes.

4. DISCUSSION

4.1. Substages of pachytene

In cultures of oocytes which had been labelled with H^3 thymidine at meiotic interphase, pachytene was estimated to last for at least eight days (4), compared with a duration of 16 days in spermatocytes (17). While the pachytene stage in the human male can be divided into seven well-defined substages on the basis of nuclear and cellular morphology (19), the situation in the female is more ambiguous. In the spermatocytes for example, the formation of prokinetochores in the centromere region and the duplication of centrioles can be followed at pachytene. The stage of development of these two structures facilitates an arrangement of pachytene spermatocytes in a temporal order. In the oocytes, a similar development of centromeres and centrioles does not take place during pachytene. Moreover, in the oocytes the development of nuclear structures exhibits considerable variation among nuclei at the same stage.

The arrangement of the pachytene oocytes into three groups is therefore based on the morphology of the chromosome bouquet, a configuration which is resolved during the pachytene stage. The contention that this subdivision reflects the development of pachytene

nuclei is supported by the observation that morphological changes of four other nuclear structures to some extent correlate with the resolution of the bouquet arrangement.

Extensive degeneration of oocytes is known to occur during the meiotic prophase in the human female (3), and the degenerating cells can easily be recognized by extreme chromatin condensation and nuclear envelope degeneration and have been excluded from this study.

4.2. Distribution of recombination nodules and bars

The bivalent complement is twice as long in oocytes as in the spermatocytes at zygotene and at pachytene (5, Table II). This difference in length, however, does not result in a corresponding increase in the number of nodules and bars in the synaptonemal complex of the female. On the contrary, more nodules were present in spermatocytes at late zygotene, than at any prophase substage of the oocytes (Table IV). This shows that the length of the synaptonemal complex per se is not a limiting factor for the binding of nodules to the synaptonemal complex.

In the oocytes, the smaller, spherical nodules develop connections to the lateral components of the synaptonemal complex and eventually, the spherical part disappears and a distinct bar bridging the central region of the synaptonemal complex remains. This transformation of nodules into bars is similar to the morphological changes reported for the spermatocytes (20), the major difference being that this morphological change in the spermatocytes starts during early pachytene, and culminates at mid pachytene. Recombination nodules and bars are eliminated during late pachytene, and by early diplotene recombination structures can no longer be detected in the spermatocytes (21). In the oocytes, nodule-bar intermediates appear already at zygotene (5), and the transformation of nodules into bars continues throughout pachytene. The maximum number of recombination bars is observed in late pachytene and early diplotene nuclei. Moreover, dissolving bars in retained central regions of the synaptonemal complex have been seen in oocytes as late as mid diplotene.

If the presence of a recombination bar indicates a crossing over event, as proposed by HOLM and RASMUSSEN (20), then in the female, an increasing number of crossing over events takes place as pachytene progresses, in contrast to the male, in which crossing over occurs mainly at mid pachytene.

The present analysis has shown that nodules and bars are distributed among the bivalents in such a way that the number of bivalents and bivalent arms without recombination structures is minimized. The observed number of bivalents devoid of a nodule or a bar is between one-third and two-thirds of the number expected if the structures were positioned by chance. The nonrandom placement is also apparent from the analysis of nodule/bar neighbour distances and nodule/bar – telomere distances, as well as from the distribution of nodule frequencies along individual bivalents. These findings are in good agreement with the general observation from a number of organisms that crossovers and chiasmata are not randomly distributed within bivalents (crossover and chiasma position interference) and that mechanisms exist which ensure each bivalent at least one chiasma. This is a prerequisite for the regular disjunction of homologues at metaphase I (32).

Similar nonrandom distributions of recombination structures have been reported from the human male (20, 27) as well as from Coprinus (22), Bombyx males (18) and Drosophila females (7, 9). The placement of nodules appeared to be random at zygotene and early pachytene and a nonrandom distribution was first observed at mid pachytene in these organisms, in contrast to the situation in human oocytes. This change in distribution pattern coincided with the transformation from one nodule type to the other in Coprinus (22), Bombyx (18) and Secale (1). In Drosophila, however, the existence of two independent nodule populations is considered (9).

As in the human male, the distribution of recombination nodules and bars along the synaptonemal complexes in the female is not uniform. Some segments receive nodules with high frequency, others rarely, still others, such as the short arms of the acrocentric chromosomes, not at all. The pattern of peaks and troughs can be related to arm lengths: short arms possess one,

intermediate arms two and long arms three to four peaks. In addition, the neighbour nodules are preferentially separated by certain distances (Figure 14). Within the bivalent arms with more than one peak, regions near the telomere exhibit higher frequency for recombination structures than interstitial segments (Figure 14).

As described in detail in section 3.7 this pattern is remarkably similar to that found in the human male, not only with respect to the number of peaks, but also with regard to the relative sizes and positions of peaks and troughs along the bivalent arms. It cannot be excluded that major differences exist within short intervals, but the overall distributions are the same. This unequivocally shows that the difference in length of the synaptonemal complex complement does not to any noticeable extent affect the distribution of recombination structures or crossing over.

4.3. Elimination of the synaptonemal complex

Synaptonemal complex segments retained after pachytene were first observed by WESTERGAARD and VON WETTSTEIN in the ascomycete Neottiella and interpreted as early chiasmata. Since then, observations in support of this contention have been obtained in a number of organisms (see 30 and 31 for review). An analysis of retained synaptonemal complex segments at early and mid diplotene in human spermatocytes, revealed that the mean number per nucleus and the distribution along the individual bivalents were similar to the estimated number of crossovers and their distribution (21). Association of recombination nodules with complex segments remaining at diplotene was reported from Sordaria (33, 34), Neurospora (15), Meloidogyne (16) and Ascaris (25). Furthermore, in the Bombyx male (18) and the basidiomycete Coprinus (22), a development of chiasmata from recombination nodules and remnants of the synaptonemal complexes was documented. In the human oocytes, the number of fragments was remarkably similar in the three nuclei investigated, despite the great differences in the total length of synaptonemal complexes. Sixty-seven and 68 synaptonemal complex segments were observed in the more advanced nuclei (no. 28 and 29). The lower number of 52 intact complex segments in the third nucleus (no. 27), which had 42 recombination nodules and bars and 78 percent of the synaptonemal complex complement intact, may be due to a less progressed state of development. Thus it seems that the initial breakdown of the complex results in formation of about 68 segments. Once this number is reached, breakdown of the central region proceeds from the ends of these segments. This number of synaptonemal complex segments is similar to a mean of 72 synaptonemal complexes, reported for human spermatocytes at early, mid and late diplotene.

In human spermatocytes, distinct synaptonemal complex segments remain associated with the chromatin of both homologues up to early diakinesis. Thereafter, the segments are shed from the bivalents and replaced by chromatin bridges by late diakinesis-prometaphase I, the released segments reassembling into synaptonemal polycomplexes in the nucleoplasm (21). In contrast, the lateral components of the oocytes remain associated with the chromatin at least up to late diplotene and structures resembling thickened lateral components were seen in oocytes from mature women (unpublished observations). The central region, however, dissolves at mid diplotene and chiasmata with a well-defined ultrastructure cannot be detected.

4.4. Assessment of the total number of crossovers

The total number of crossovers can be determined from two sources, namely from the cumulated distributions of recombination structures and from the number of synaptonemal complex fragments temporarily retained between the homologues during part of diplotene. In the human male, light microscopic data on the number and distribution of chiasmata (23) have shown that 95 percent of the short arms of bivalents 17-20 and the long arms of bivalents 16-19 get one chiasma. If the mean cumulated frequency of recombination structures on these arms is used as a standard for one crossover, the total number of crossovers per nucleus then amounts to 69. As chiasma frequencies for individual bivalent arms are not available for

the female, the same standards cannot be used for estimating the total number of crossovers in the female. A minimum estimate can, however, be obtained if one assumes that each long arm of the two shortest bivalents gets one crossover (the number of chiasmata reported for bivalents 21 and 22 ranges from 1.00 to 1.11 (24) in reasonable agreement with this assumption). Using a mean cumulated frequency of recombination structures (4.37) as measure of one crossover, the total number of crossovers per oocyte amounts to 53 i.e., the total cumulated frequency of 233 divided by 4.37.

It should be pointed out that both estimates depend on the assumptions that 1) the lifetime of recombination structures is constant in each sex, 2) that the fraction of recombination structures which actually leads to a crossover is the same in all bivalent arms and 3) that the crossing over frequencies assigned to the bivalent arms used as standards are correct.

As pointed out in section 4.3, a segment of the synaptonemal complex is retained at the site of the early chiasma in a number of organisms (31). In the human male it was shown that the number of temporarily retained pieces of synaptonemal complex at diplotene corresponded to the number of crossovers estimated from the recombination structures. This numerical similarity was considered a strong indication that in the human male the total number of crossovers per nucleus is about 70 (69 determined from recombination structures and 72 determined from retained pieces of synaptonemal complex).

In the reconstructed diplotene oocytes, 67 and 68 pieces of synaptonemal complex remained. Taking these values as indicative of the total number of crossovers per nucleus, the value then ranges between 53 (determined from recombination structures) and 68 (determined from retained synaptonemal complex segments). It can thus be concluded that the total frequency of crossing over is either similar in the two sexes or slightly lower in the female.

The crossing over frequencies estimated above exceed considerably the mean of 43.5 chiasmata, reported for diakinesis/metaphase I bivalents (24) and are higher than the chiasmata counts (range 37 to 48) seen in fifteen oocytes matured in vitro (13). As in the male, the differences between the frequency of crossovers estimated from the ultrastructural analyses and the mean number of chiasmata observable in the light microscope at diakinesis can be attributed to a reduction in chiasma frequency by terminalization.

ACKNOWLEDGEMENTS

I am indebted to SØREN W. RASMUSSEN and PREBEN B. HOLM for scientific and practical guidance and encouragement throughout this work. Their and DITER VON WETTSTEIN'S valuable criticism of this communication is also highly appreciated. Expert technical assistance was provided by JEAN SAGE, DAN OLSSON and NINA RASMUSSEN. FRANS BIERRING, MOGENS RØNNE, JØRGEN GRINSTED and ULLA HAUSCHILD are thanked for their assistance in obtaining the ovaries. This work was financially supported by grant BIO-E-417-DK-G from the Commission of the European Communities to D. VON WETTSTEIN.

REFERENCES

1. ABIRACHED-DARMENCY, M., D. ZICKLER & Y. CAUDERON: Synaptonemal complex and recombination nodules in rye (Secale cereale). Chromosoma (Berl.) 88, 299-306 (1983)
2. ANDERSSON, L. & K. SANDBERG: Genetic linkage in the horse. II. Distribution of male recombination estimates and the influence of age, breed and sex on recombination frequency. Genetics 106, 109-122 (1984)
3. BAKER, T.G.: A quantitative and cytological study of germ cells in human ovaries. Proc. Roy. Soc. B. 158, 417-433 (1963)
4. BAKER, T.G. & P. NEAL: Oogenesis in human fetal ovaries maintained in organ culture. J. Anat. 117, 591-604 (1974)
5. BOJKO, M.: Human meiosis VIII: Chromosome pairing and formation of the synaptonemal complex in oocytes. Carlsberg Res. Commun. 48, 285-305 (1983)
6. CALLAN, H.G. & P.E. PERRY: Recombination in male and female meiocytes contrasted. Philos. Trans. R. Soc. Lond. B. 277, 227-233 (1977)
7. CARPENTER, A.T.C.: Electron microscopy of meiosis in Drosophila melanogaster II. The recombination nodule – a recombination associated structure at pachytene. Proc. Nat. Acad. Sci. USA 72,

3186-3189 (1975)
8. CARPENTER, A.T.C.: Recombination nodules and synaptonemal complex in recombination-defective females of Drosophila melanogaster. Chromosoma (Berl.) 75, 259-292 (1979)
9. CARPENTER, A.T.C.: Synaptonemal complex and recombination nodules in wild-type Drosophila melanogaster females. Genetics 92, 511-541 (1979)
10. CARPENTER, A.T.C.: EM autoradiographic evidence that DNA synthesis occurs at recombination nodules during meiosis in Drosophila melanogaster females. Chromosoma (Berl.) 83, 59-80 (1981)
11. COOK, P.J.L.: The Lutheran-Secretor recombination fraction in man: a possible sex difference. Ann. Hum. Genet. Lond. 28, 393-401 (1965)
12. DUNN, L.C. & D. BENNETT: Sex differences in recombination of linked genes in animals. Genet. Res. Camb. 9, 211-220 (1967)
13. EDWARDS, R.G.: Observations on meiosis in normal males and females in human population cytogenetics. Ed. P.A. Jacobs, W.H. Price, P. Law. Pfizer Medical Monographs 5. Edinburgh, p. 9-21 (1970)
14. FERGUSON-SMITH, M.A.: Meiosis in the human male. In: Chromosomes Today. Vol.5. Eds.: P.L. Pearson & K.R. Lewis. John Wiley & Sons, New York, pp 33-41 (1976)
15. GILLIES, C.B.: The relationship between synaptonemal complexes, recombination nodules and crossing over in Neurospora crassa bivalents and translocation quadrivalents. Genetics 91, 1-17 (1979)
16. GOLDSTEIN, P. & A.C. TRIANTAPHYLLOU: Occurrence of synaptonemal complexes and recombination nodules in a meiotic race of Meloidogyne hapla and their absence in a mitotic race. Chromosoma (Berl.) 68, 91-100 (1978)
17. HELLER, C.G. & Y. CLERMONT: Kinetics of the germinal epithelium in man. Recent Prog. Horm. Res. 20, 545-575 (1964)
18. HOLM, P.B. & S.W. RASMUSSEN: Chromosome pairing, recombination nodules and chiasma formation in diploid Bombyx males. Carlsberg Res. Commun. 45, 483-548 (1980)
19. HOLM, P.B. & S.W. RASMUSSEN: Human meiosis V. Substages of pachytene in human spermatogenesis. Carlsberg Res. Commun. 48, 351-383 (1983)
20. HOLM, P.B. & S.W. RASMUSSEN: Human meiosis VI. Crossing over in human spermatocytes. Carlsberg Res. Commun. 48, 385-413 (1983)
21. HOLM, P.B. & S.W. RASMUSSEN: Human meiosis VII. Chiasma formation in human spermatocytes. Carlsberg Res. Commun. 48, 415-456 (1983)
22. HOLM, P.B., S.W. RASMUSSEN, D. ZICKLER, B.C. LU & J. SAGE: Chromosome pairing, recombination nodules and chiasma formation in the basidiomycete Coprinus cinereus. Carlsberg Res. Commun. 46, 305-346 (1981)
23. HULTÉN, M.: Chiasma distribution at diakinesis in the normal human male. Hereditas 76, 55-78 (1974)
24. JAGIELLO, G., M. DUNCAYEN, J.-S. FANG & J. GRAFFEO: Cytogenetic observations in mammalian oocytes. In: Chromosomes Today, Vol. 5. Eds.: P.L. Pearson and K.R. Lewis. John Wiley & Sons, New York, pp 43-63 (1974)
25. KUNDU, S.C. & YU.F. BOGDANOV: Ultrastructural studies of late meiotic prophase nuclei of spermatocytes in Ascaris suum. Chromosoma (Berl.) 70, 375-384 (1979)
26. RASMUSSEN, S.W.: The meiotic prophase in Bombyx mori females analyzed by three dimentional reconstructions of synaptonemal complexes. Chromosoma (Berl.) 54, 245-293 (1976)
27. RASMUSSEN, S.W. & P.B.HOLM: Human meiosis II. Chromosome pairing and recombination nodules in human spermatocytes. Carlsberg Res. Commun. 43, 275-327 (1978)
28. RASMUSSEN, S.W. & P.B. HOLM: Mechanics of meiosis. Hereditas, 93, 187-216 (1980)
29. WEITKAMP, L.R., J.J. VAN ROOD, E. THORSBY, W. BIAS, M. FOTINO, S.D. LAWLER, J. DAUSSET, W.R. MAYR, J. BODMER, F.E. WARD, J. SEIGNALET, R. PAYNE, F. KISSMEYER-NIELSEN, R.A. GATTI, J.A. SACHS & L.U. LAMM: The relation of parental sex and age to recombination in the HL-A system. Human Heredity 23, 197-205 (1973)
30. WESTERGAARD, M. & D. VON WETTSTEIN: The synaptinemal complex. Ann. Rev. Genet. 6, 71-110 (1972)
31. WETTSTEIN, D. VON, S.W. RASMUSSEN & P.B. HOLM: The synaptonemal complex in genetic segregation. Ann. Rev. Genet. 18, 331-413 (1984)
32. WHITEHOUSE, H.L.: Genetic recombination. Understanding the mechanisms. Chichester, John Wiley & Sons (1982)
33. ZICKLER, D.: Development of the synaptonemal complex and the "recombination nodules" during meiotic prophase in the seven bivalents of the fungus Sordaria macrospora Auersw. Chromosoma (Berl.) 61, 289-316 (1977)
34. ZICKLER, D. & J. SAGE: Synaptonemal complexes with modified lateral elements in Sordaria humana: Development of and relationship to the "recombination nodules". Chromosoma (Berl.) 84, 305-316 (1981)

Accepted by: H. KLENOW, E. LUND and S.O. ANDERSEN